INTERDISCIPLINARY DOCTORAL SCHOOL

Faculty of Mechanical Engineering

Drd. Ing. Florin DUMBRAVĂ

Research on the modeling, simulation and testing of elements in the construction of thin-walled metallic structures

SUMMARY

Scientific supervisor

Prof.Dr. Ing. Camelia CERBU

BRAȘOV, 2024

FOREWORD

I would like to extend my deepest gratitude to Professor Camelia Cerbu for her invaluable support. Without her assistance and patience, the completion of my doctoral studies would not have been possible. I am profoundly grateful for her scientific guidance, constructive suggestions, and the support she provided in completing this work, as well as for her collaboration in the publication of articles. I hope she will also take pride in our shared achievements.

I wish to express my appreciation to the guidance committee (Prof. Dr. Ing. Sorin Vlase, Prof. Dr. Ing. Vasile Ciofoaia, Prof. Dr. Ing. Ioan Călin Roșca, and Assoc. Prof. Dr. Ing. Florin Baciu) for their valuable guidance and advice throughout the entire process of developing my doctoral thesis.

In particular, I would like to thank Dean Ioan Călin Roșca for his support.

I wish to pay tribute to my professors, especially Professor Ioan Curțu, whom I hold in the highest regard. He instilled in me a passion for material strength and structural analysis and has been an essential mentor in my professional journey. I am grateful for the inspiration and enthusiasm he has shared with me.

I express my profound gratitude to Brian Howson, with whom I have had the privilege of working for over 10 years at Dexion Storage Solutions. As a true supporter of Romania and an exemplary professional, he has had a significant impact on my professional and personal development. I am deeply thankful for the trust he has placed in me and for his support in enhancing my skills as an engineer. I hope to extend the same confidence and support to others that I have received from him.

I would also like to express my appreciation to my colleagues, particularly Mr. Marian Ioniță, whose extraordinary intelligence has provided me with daily opportunities for learning.

I wish to express my gratitude to my family, especially my mother, Ioana Dumbrava, who has provided unwavering support throughout all stages of my life and has been a true pillar of strength. I am aware that many people have contributed to my journey, and although I cannot mention everyone individually, I want to assure them all of my profound gratitude for their role in my development.

I would like to thank everyone who has supported me, especially during the most challenging times.

To my daughter Ingrid, I send all my love and apologize for the time I could not spend with her due to my commitment to my studies. I hope that as she grows up, she will be proud of me and the effort I have put in.

CONTENT

1. INTRODUCTION

1.1 Relevance and Importance of the research topic

Pallet rack storage systems are a crucial component of modern logistics, facilitating the efficient and accessible storage of goods across various industries. With the rapid growth of e-commerce and logistics, the demand for efficient and well-organized storage spaces has increased significantly. Metal storage structures, such as pallet racks, play a vital role in optimizing storage space and enabling quick access to goods.

The safety of metal structures is essential for preventing accidents and damage to stored goods. Research into improving joints and structural components contributes to the development of safer and more reliable storage systems. The specialized literature recognizes the importance of analyzing the structural behavior of these connections. Previous studies have demonstrated that rotational stiffness and bending capacity of joints have a significant impact on displacements and stresses in rack systems. However, there are still contradictory and insufficiently explored aspects, particularly regarding the influence of column thickness and connector type on these connection characteristics between beams and columns. Advances in manufacturing technology and the use of advanced materials, such as high-strength steels, necessitate constant updates to design and testing methods for structures. Ongoing research ensures the integration of these innovations into storage solutions.

Adhering to current norms and regulations requires adopting design and testing practices based on the latest knowledge and standards. Research contributes to the development and updating of these norms, ensuring that metal structures comply with legal and safety requirements. Cost efficiency in the production and installation of metal structures is a crucial aspect for logistics and storage companies. Research studies can identify more economical and cost-effective solutions without compromising quality and safety. Developing sustainable storage solutions that use resources efficiently and reduce environmental impact is another important reason for the research topic. Using recyclable materials and reducing the carbon footprint are essential goals in modern metal structure design.

The widespread use of pallet rack storage systems highlights the need for a deeper understanding of the effects of interactions between metallic pins in connectors and column perforations on the performance of load-bearing beams. Although some studies have addressed this topic, the results are not always conclusive, indicating the need for further investigation. In this context, this paper aims to fill gaps in the specialized literature through an objective and detailed analysis of the mechanical behavior of semi-rigid connections used in storage systems. The study will focus on investigating the effects of column thickness and the type of metallic pin connector on rotational stiffness and bending moment capacity of the tested connections. Additionally, it will explore the impact of geometric imperfections on the stability and critical buckling forces of columns made from Omega-shaped profile sections under compression.

This research aims to provide a comprehensive and critical perspective on the analyzed issues, contributing to the development of more accurate and efficient models for designing and simulating the mechanical behavior of components in storage systems. Advanced numerical simulation methods and experimental tests will be used to validate and calibrate the proposed models, ensuring the relevance and applicability of the obtained results.

1.2 Content of the thesis

The first three chapters of this thesis present the justification for the choice of research topic and the context leading to the necessity of conducting the research outlined in the doctoral thesis. A synthesized classification of storage systems is provided, including the structural components of pallet rack structures, types of joints and columns used, manufacturing technologies, as well as conclusions and issues identified within this industry. The importance of the connections between beams and columns in ensuring the stability and safety of storage structures is highlighted. Additionally, the current state of research in the specialized literature is reviewed, examining the norms and design codes applied to such structures, theoretical aspects, and current research related to joints between beams and columns, compression of thin-walled columns with Omega-shaped cross-sections, emphasizing areas that require further studies. A review of the specialized literature is conducted to identify existing gaps in research on such structures, justifying the motivation for choosing the research topic for the doctoral thesis.

Chapter 4 elaborates on the main objectives of the thesis, as well as the specific objectives derived from them.

Chapters 5 and 6 focus on research concerning the rotational stiffness of joints with metallic connectors and pins. The experimental effects of the structural parameters of the beam-to-column connection on the rotational stiffness of these connections are studied, analyzing different modes of failure and the impact of rotational stiffness on the mechanical behavior of the beams. The effect of play in pin connector joints on sectional forces and beam displacements is also investigated based on experimental results and calculations. The effects of rotating the connector to eliminate play, as well as the impact of connector rotational stiffness on the structural performance of storage systems, are analyzed.

Chapter 7 presents experimental research and numerical simulations concerning the local stability loss of short columns made from thin-walled profiles. The main geometric characteristics of the columns, testing methods, obtained results, and conclusions from the tests performed are presented. Experimental determination of the critical buckling forces and effective area for columns made from thin-walled Omega-shaped profiles is conducted.

Chapter 8 is dedicated to the general conclusions of the doctoral thesis, the author's personal contributions, and potential future research directions for improving and developing metal storage structures. The importance of continuing research to address future challenges and enhance the performance of storage systems is emphasized.

2. CURRENT REQUIREMENTS AND SOLUTIONS FOR THE CONSTRUCTION OF METAL PALLET RACK STRUCTURES

2.1 Classification of storage systems

Storage systems are generally metal structures designed for storing goods in warehouses or commercial spaces. They are typically classified into two main categories:
- Pallet Racking System.
- Shelving Systems.

The primary difference between these two types of systems is that, in the first case, pallets are used to store goods, whereas in the second case, the systems are generally intended for storing small items that can be handled manually.

Pallet racking systems are further classified into various types, which may offer higher space efficiency or cost-effectiveness. The main types are as follows:
- Conventional Pallet Racking Systems.
- Drive-In Racking Systems.
- Pallet Shuttle Racking Systems.
- Pallet Flow Racking Systems.
- Mobile Pallet Racking Systems.
- Crane-Handled Pallet Racking Systems.

Each type is discussed in detail with examples. Figure 2.1 illustrates conventional pallet racking systems.

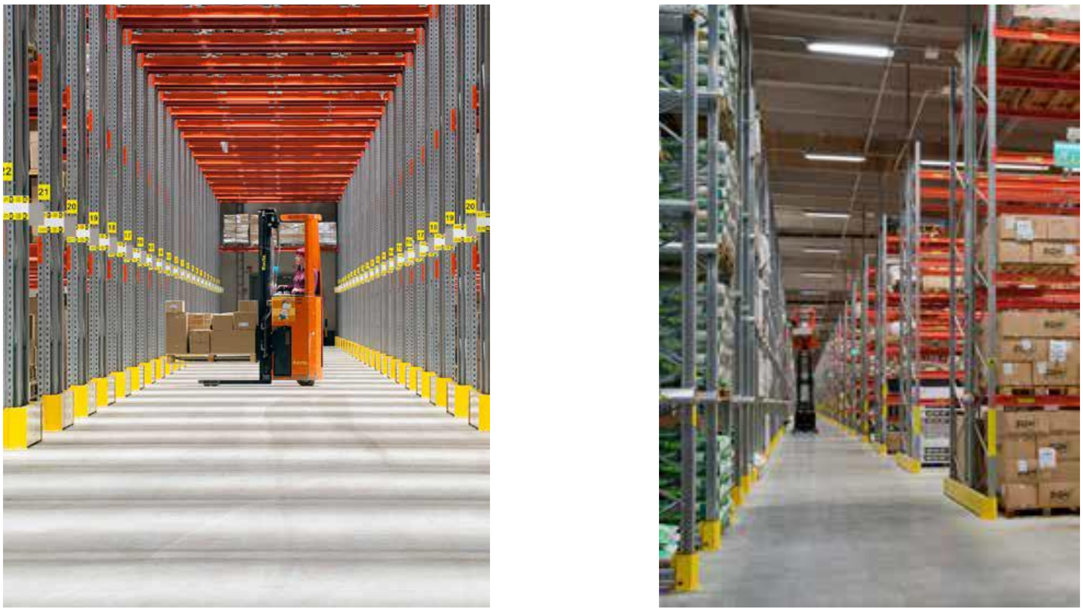

(a) (b)

*Figure 2.1. Conventional Pallet Racking Systems (***a, 2019).*

These types of systems ensure unrestricted access to all pallets at any time. Access to the pallets is achieved using a forklift. The load-bearing structure of this type of system consists of horizontal elements called beams, which are equipped with metal connectors at their ends. These connectors link the horizontal elements to the vertical elements (frames), which in turn are composed of columns and braces. At the base of the columns, there are so-called base plates, which connect the structure to the floor (see Fig. 2.2).

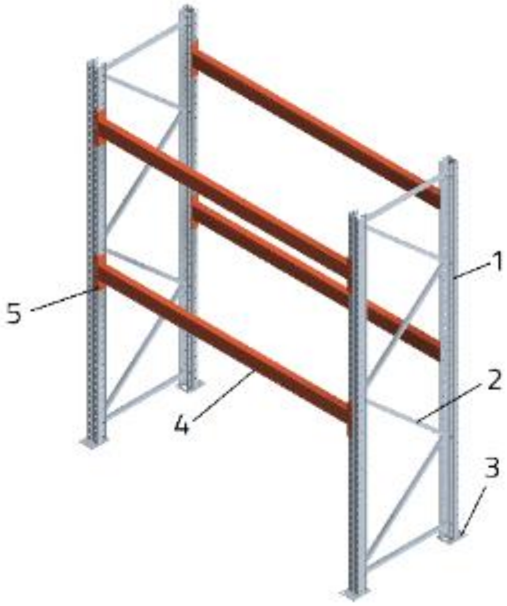

Figure 2.2. Constitutive Elements of a Frame: 1-Column; 2-Diagonal Elements (Braces); 3-Base Plate; 4-Beam; 5-Connector.

Figure 2.3 shows several "Drive-In" pallet racking systems.

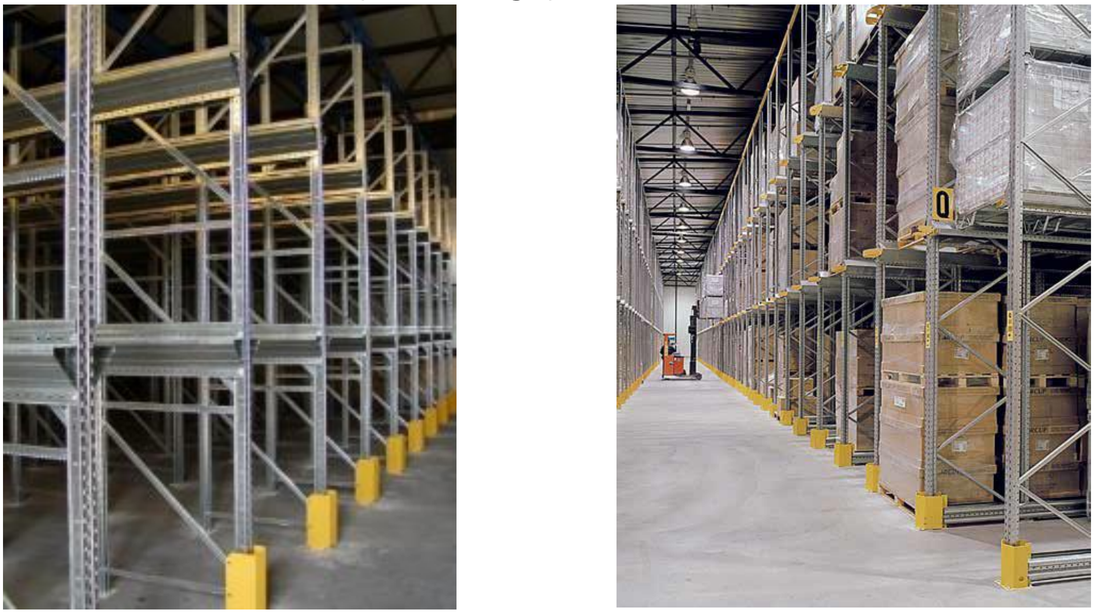

(a) (b)

*Figure 2.3. Drive-In Racking Systems (***a, 2019).*

These types of systems are designed so that the forklift can access the interior of the rack, navigating through the rows created by the frames mentioned earlier. In this case, however, the pallets are not positioned on beams but on rails connected to the frames.

Figure 2.4 presents an example of a pallet racking system with an automatic shuttle (radio-controlled shuttle). In English, this storage system is referred to as a "pallet shuttle." This is a semi-automated storage solution for pallets. Pallet handling within the rack is accomplished using automated shuttles.

*Figure 2.4. Pallet Shuttle Racking Systems (***a, 2019).*

Figure 2.5 shows an example of a FIFO (First In, First Out) pallet racking system with roller conveyors.

*Figure 2.5. Pallet Flow Racking Systems (***a, 2019).*

In this system, pallets move on rollers. Pallets at the front are picked up from the front of the rack, while new pallets are stored at the rear. The movement of pallets within the rack is smooth due to automatic braking. This system significantly improves the efficiency of the warehouse space compared to conventional racking systems.

Figure 2.6 shows an example of a mobile pallet racking system.

*Figure 2.6. Mobile Pallet Racking Systems. (***a, 2019).*

The mobile racking system is a dynamic system consisting of two main parts: the mobile base of the rack and the rack itself, which is generally the same type of rack used in conventional versions. The mobile base moves on tracks embedded in the floor, and the operation is controlled electronically. This system represents one of the most efficient solutions in terms of space savings.

Figure 2.7 shows pallet racking systems where pallet handling is done with cranes.

*Figure 2.7. Crane-Handled Pallet Racking Systems (***a, 2019).*

This type of racking belongs to the category of semi-automated or fully automated dynamic systems. They are generally used in storage systems with heights up to 25 meters. Cranes are integrated into the warehouse management system and can move up to 200 pallets per hour.

2.2 Constructive elements of metal racking structures

The load-bearing structure for these types of metal racks is generally made from cold-rolled steel. The main elements of these structures are:

- Beams
- Columns (Uprights)
- Bracing

Beams are composed of two "C" profiles assembled together (see Fig. 2.8a), which are equipped with metal connectors with pins at their ends (see Fig. 2.8b and Fig. 2.8c). The connectors can be joined to the beams either by welding or through other methods, such as bolts or other devices (hooks or pins), which facilitate the connection with the vertical columns via the perforations on their front side.

(a) (b) (c)

Figure 2.8. Beam's elements:(a) Cross-section of the beam formed by joining two C profiles;(b) Connector; (c) Assembly consisting of a beam and two connectors.

Uprights are the vertical elements of the structure and generally have an Omega (Ω) cross-section. They are equipped with perforations on the front side and holes on the side flanges. The perforations allow for the connection with connectors fixed to the ends of the beams, while the side holes facilitate the attachment of bracing using bolts.

(a) Upright (b) Bracing (c) Frame

Figure 2.9. Frame configurations (a) upright; (b) bracing; (c) frame assembled from bracing and uprights.

In addition to supporting vertical loads, the beams ensure stability in the aisle direction (Dumbrava and Cerbu, 2020b) between the storage systems, referred to as "Down Aisle – D.A." in English-language literature. In this context, the design of the connection between the beam and the upright (see Fig. 2.10a) is of major importance.

Stability in the aisle direction is also influenced by the connections between the base plate and the upright (see Fig. 2.10b).

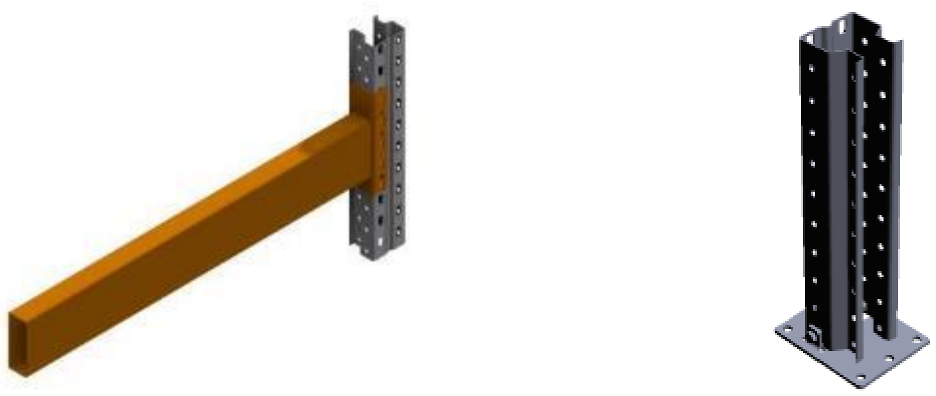

(a) (b)

Figure 2.10. Connections in Storage Systems: (a) Connection between the beam and the upright; (b) Connection between the upright and the base plate.

The stability of the structure in the direction perpendicular to the aisle, known in the literature as "Cross Aisle," is provided by the frame formed by the uprights and bracing. There are several types of frames, depending on the arrangement of the bracing, as shown in Figure 2.11.

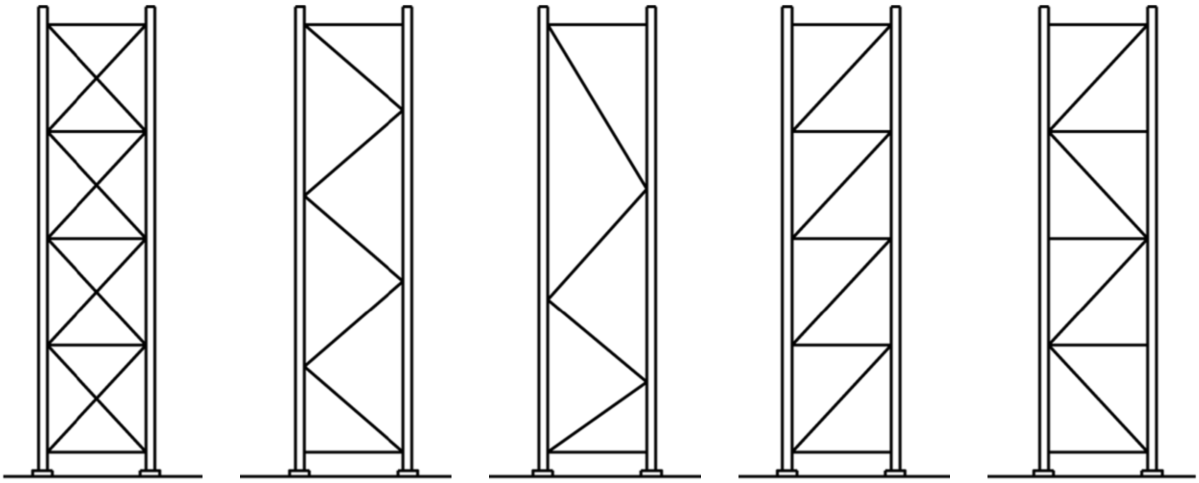

(a) (b) (c) (d) (e)

*Figure 2.11. Types of Braced Frame Configurations: (a) Frame with Tension Bracing; (b) **Frame with Regular "D" Bracing; (c) Frame with Irregular "D" Bracing; (d) Frame with "Z" Bracing; (e) Frame with "K" Bracing.*

2.3 Types of connections used in metal racking structures

The following section will present a classification of the main types of connections, as well as a classification of the different shapes of columns used in the construction of pallet racking storage systems.

- Connections with metal connectors with pins
- Connections with metal connectors with pins and bolts
- Connections used in cantilever beams
- Connections with end plates and bolts

2.4 Types of columns used in metal racking structures

The most common cross-section shape used for columns in these types of structures is the omega (Ω) shape. There is a considerable variety of columns with this type of cross-section, each with distinct characteristics. The main differences between them include:

- The configuration of the perforations on the front of the columns, which facilitates the connection of beams to columns using pin connectors; usually, each supplier of such construction solutions uses a specific type of perforation, which becomes a distinctive mark for each manufacturer.
- The shape of the column's cross-section.
- The type of steel used.

There are various geometric shapes of perforations, typically located on the front of the columns. The geometric shape and position of the perforations are some of the defining features of the columns. A different shape will also require special metal pins to ensure proper connection with the beams. The geometry and dimensions of the perforations affect the stability of the columns, particularly their effective area.

- Types of geometric shapes for column perforations

Figure 2.17 presents several perforation shapes encountered among some of the leading suppliers of such systems in Europe and other regions.

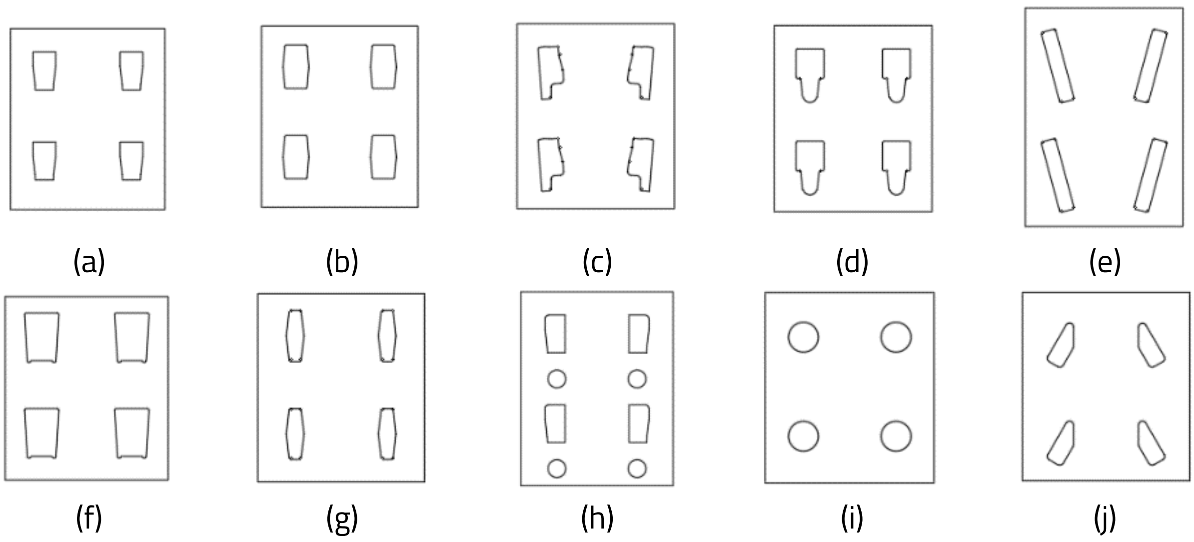

Figure 2.17. Shapes of perforations present on the front side of columns

- Different geometries of column profiles

One of the most important characteristics for determining the strength of these types of columns is their geometric cross-sectional shape (see Fig. 2.18).

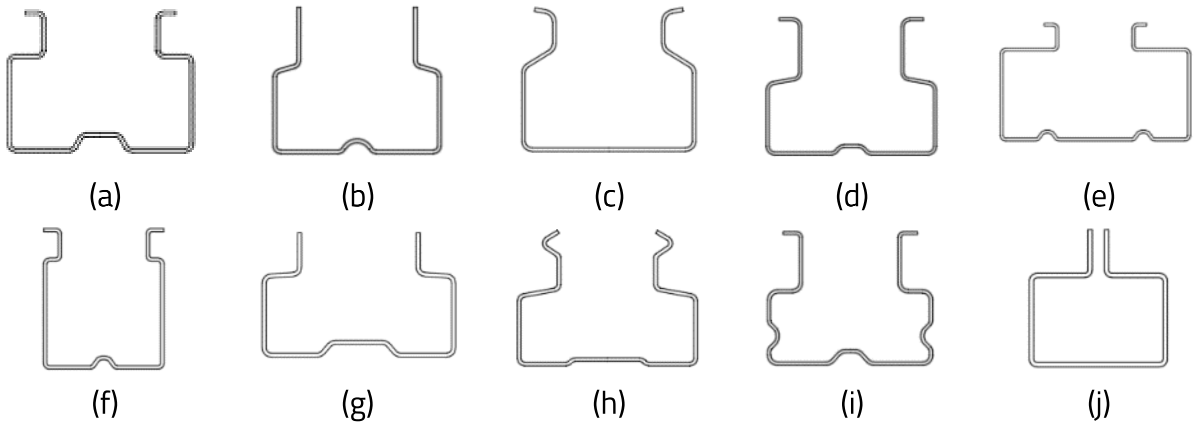

Figure 2.18. Types of cross-sections for omega columns

2.5 Aspects of manufacturing technology for storage structure elements

The manufacturing process used for producing beams in storage structures is known as cold rolling or cold forming. The technology for manufacturing cold-formed elements can be carried out using one of the following two methods:

- Cold Rolling: This process involves passing the steel through rollers at room temperature to achieve the desired cross-sectional shape. Cold rolling increases the strength and hardness of the material through deformation.
- Cold Bending: This technique involves bending the steel at room temperature to achieve the desired shape. It is often used to create complex profiles and geometric forms.

Both methods are employed to create structural elements with precise dimensions and enhanced mechanical properties, crucial for the stability and performance of storage systems.

2.6 Conclusions

Cold-formed metal profiles are widely used in storage systems, providing a variety of shapes required in the industry. In Romania, Dexion Storage Solutions is a leading producer of these structures, consuming approximately 18,000 tons of steel in 2023. The study focuses on theoretical and experimental research concerning columns and connections between beams and columns, both produced through cold rolling. The columns have wall thicknesses up to 5 mm, while the beams have thicknesses up to 3 mm.

Compared to sections obtained through hot rolling or welding, thin-walled profiles with open contours, used for beams and columns, present complex structural issues. The steels used have high yield strengths, ranging from 320 MPa to over 500 MPa. Reducing the steel thickness, combined with using high-strength steels, can lead to stability loss in structures due to wall buckling and global buckling, thereby affecting the material's ductility.

These conclusions underscore the importance of considering both the material properties and the structural design when using cold-formed profiles in storage systems to ensure stability and performance.

3. . CURRENT STATE OF RESEARCH ON MODELING AND TESTING OF COMPONENTS IN METAL STORAGE STRUCTURES

3.1 Standards and design codes used for calculating metal storage structures

To provide an overview of the most important structural design guidelines for storage structures, it is essential to understand the specifics of these types of structures based on several criteria presented below:

Materials and Sections: Metal structures used for pallet storage are generally made from cold-rolled steel, resulting in thin-walled sections with open contours, which feature perforations along their length, influencing the geometric characteristics of the sections.

Symmetry and Buckling: The profiles are symmetrical only with respect to one axis, making them prone to buckling through twisting (twisting around the shear center of the section).

Stability and Strength Limits: Stability loss can occur before the element reaches its strength limit.

Connections: Special connections are used between the structural elements, exhibiting semi-rigid behavior.

Eccentricities: Various eccentricities between elements arise, which are generally neglected by European standards concerning traditional steel structures.

Calculation Methods: Calculation methods are based on experimental tests due to the specific characteristics of sections, which differ significantly from one manufacturer to another.

All these aspects have led to the development of specific design guidelines for the structural calculation of storage structure components.

In Europe, since 2020, the standard EN 15512 (2020) has been in use. This standard provides principles for the structural calculation of storage structures. The need for this standard arose from the desire to unify the calculation principles used by major racking manufacturers in Europe. This standard is based on the FEM 10.2.02 design code developed by FEM – European Materials Handling Federation, which subsequently led to the European standard (EN 15512, 2009), revised in 2020 (EN 15512, 2020).

Efforts have been made to correlate the principles presented in the standard (EN 15512) with relevant European codes for calculating thin-walled sheet structures.

Therefore, these standards offer a unified and detailed framework for designing and calculating storage structures, considering the specificities and complexities of these types of structures.

In the field of metal storage structures, which differ significantly from traditional steel constructions, specific standards and design codes apply. These standards consider the structural and performance characteristics of these systems, ensuring their safety and efficiency. The complete thesis specifies the standards used in the design of metal storage rack structures.

ge systems.

These standards and codes are essential for the proper design and use of metal storage structures, providing clear guidelines and safety standards for engineers and designers.

These standards and codes offer a detailed and coherent framework for the design and assessment of storage structures, ensuring compliance and safety in their use.

The European standard EN 15512:2009 has been revised and replaced with EN 15512:2020, a process coordinated by the working group within Technical Committee 344 (CEN TC344). The Romanian Standardization Association (ASRO) is also represented in this working group at the European level.

The new EN 15512 standard aims to align calculation principles as closely as possible with other relevant European standards, which are also undergoing revision.
In the United Kingdom, in addition to EN 15512, the SEMA – Code of Practice for Design of Adjustable Pallet Racking is used. The latest version of the SEMA code, available since 2014, is based on the British standard BX5950 - Structural Use of Steelwork in Building. Code of Practice for Design. Rolled and Welded Sections. The SEMA code offers a number of simplifications compared to the principles presented in the European standard EN 15512 (2020). It first appeared in 2008, and the current version differs slightly from the previous one.
In Australia, the AS 4084 – Steel Storage Racking standard, introduced in 2012, is used. This standard is based on the European standard EN 15512, version 2009. Although there are numerous similarities between EN 15512 and AS 4084, significant changes have been made to adapt to local requirements.
In the United States, the ANSI MH16.1 standard is used, last revised in 2023. This is an updated version of the first edition that appeared in 2012. The development was based on the procedures established by the Material Handling Industry (MHI) and was carried out by the Rack Manufacturers Institute (RMI).

3.2 Theoretical and experimental aspects of beam-to-column connections used in the metal racking industry

All design codes and standards that establish calculation principles for these types of structures detail methods for obtaining the mechanical characteristics of elements through experiments. In this chapter of the doctoral thesis, the experimental-assisted calculation method for determining the rotational stiffness of the joint between beam and column, as well as for determining the design moment of the joint used in the construction of metal structures for pallet storage, is presented.
The experimental method is described in detail in the European standard EN 15515 (2020), and Figure 3.1 illustrates the loading scheme specific to this type of experiment.

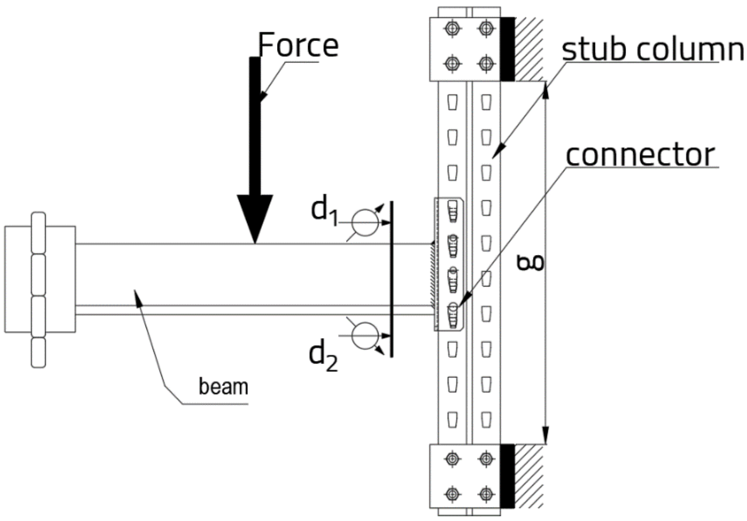

Figure 3.1. Testing scheme for Beam End Connector Test

The European Standard EN 15512 (2020) also specifies the method for evaluating rotational stiffness and design moment capacity.

The experimental method involves determining the rotation-moment curve, as shown in Figure 3.2. This curve is crucial for understanding how the joint behaves under load and is essential for accurate structural design.

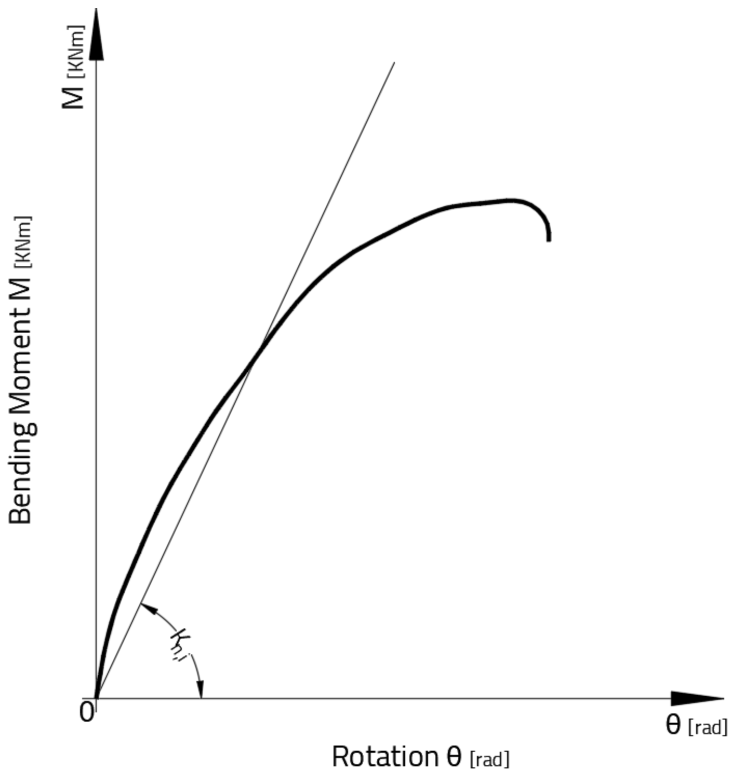

Figure 3.2. Obtaining Rotational Stiffness According to EN 15512

The results obtained are then integrated into the global analysis of pallet racking systems.
For analytical calculation, the following relationships are used:

$$M_{con} = \frac{qL^3}{24EI_z\left(\frac{1}{k_m} + \frac{L}{2EI_z}\right)}; \tag{3.5}$$

$$M_{mij} = \frac{qL^2}{8} - M_{con}; \tag{3.6}$$

$$v_{max} = \frac{qL^4(10EI_z + Lk_m)}{384EI(2EI_z + Lk_m)}, \tag{3.7}$$

In which M_{con} and M_{mij}represent the bending moments developing at both ends of the beam at the semi-rigid connections and the bending moment developing at the midpoint of the beam, respectively; $L$is the length of the beam; $E$is the longitudinal modulus of elasticity; I_z is the moment of inertia of the beam's cross-section with respect to the neutral axis; k_m denotes the rotational stiffness of the end connection; and v_{max} is the maximum deflection at the midpoint of the beam.

The derivation of equations (3.5), (3.6), and (3.7) is presented in detail in Appendix 2 of the thesis.

3.3. Current research on beam-to-column connections in steel racking systems

In recent years, there has been a significant increase in consumption, leading to a rise in the production of storage rack systems. Products are often stored in pallet racking systems in supermarkets or in warehouses for products or raw materials within factories.

Pallet racking systems are self-supporting structures that must bear substantial vertical loads. They are generally composed of two main types of components: frames and beams. The frames are made from vertical thin-walled profiles with perforations along their entire length, which facilitate connections with the beams, typically using metal connectors with pins (Shariati et al., 2018; Zhao et al., 2014). These connectors are welded to both ends of the beams. Horizontal and diagonal bracing welded between the uprights (columns) ensures the stability of the frame in the transverse direction. Beams provide stability in the longitudinal direction, and the rigidity of the connections is a crucial characteristic of storage racking systems in this context.

In addition to metal connectors with pins, there are other types of connections used in construction, including metal connectors with bolts or screws (Dai et al., 2018a), wood-steel-wood connections with external parts made of wood and an internal steel component (Elza and Pedro, 2020), and pin connectors combined with additional fastening by bolts (Gusella et al., 2018). The latter type of connection is commonly known as "speed lock" connections (Dai et al., 2018b).

In simple terms, the connections used between beams and uprights (columns) are either pinned or rigid. In practice, for nearly all connections, even those considered rigid, there can be some rotations affecting internal forces, particularly bending moments. Not all connections deemed rigid are completely rigid in reality. Conversely, connections considered pinned are not perfectly pinned due to friction that affects the rotation of the connection. Therefore, estimating the stiffness of connections becomes necessary, especially for those used in pallet racking structures.

With the introduction of EN 1993-1-3, Eurocode 3 (EC3-3, 2006), a classification of connections used between beams and uprights based on their stiffness was established. The connections investigated in this research fall into the category of semi-rigid connections. The stiffness of these connections is determined experimentally, according to standard EN 15512 (EN 15512, 2009). It is essential to understand that determining the rotational stiffness of the connections and the capable bending moment is crucial; otherwise, pallet racking systems may not function safely.

Theoretically, some researchers have proposed in recent publications (Zhao et al., 2017; Gusella et al., 2018; Gusella et al., 2019) a mechanical model that includes five basic deformable components (bending metal pins, the column profile wall subjected to shear force and bending, the metal pin connector in bending and shear) of beam-to-column connections to evaluate the initial rotational stiffness of the connections.

Regarding beams used for storage racking systems, since they are cold-formed thin-walled steel structural elements, distortional buckling failures may occur in bending, and the effects of shear force need to be accurately evaluated in bending, especially for thin-walled elements with open sections (Degtyareva and Degtyarev, 2016; Degtyareva, 2017). An interesting study (Degtyarev and Degtyareva, 2016) presents results on elastic buckling loads and ultimate strength using numerical simulations of stresses and deformations in finite element models of cold-formed C-profiles with slots subjected to shear.

3.4. Theoretical aspects of column compression

First, we present the columns with a cross-section shaped like the letter omega (Ω), as they are the focus of this study.

Columns with an omega (Ω) shaped cross-section are made from thin steel sheets, usually up to four or even five millimeters thick, though in general, thinner sheets, even as little as one and a half millimeters, are used. Due to the shape of the cross-section, the shear center is offset from the center of mass, which makes the profile sensitive to torsion (see Fig. 3.15).

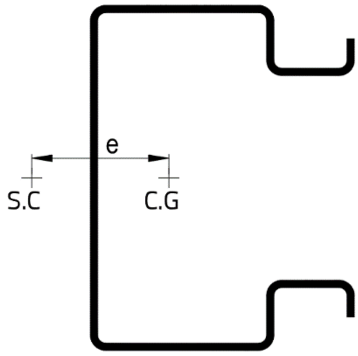

C.G - Center of gravity
S.C - Shear center
e - eccentricity

Figure 3.15. Distance Between the Center of Gravity and the Shear Center of an Omega Column Section.

Depending on the slenderness of the bar and the critical force or moment, three main types of buckling are distinguished:

- Short Columns: Characterized by local and/or distortional buckling. These are bars where the length is relatively short compared to their cross-sectional dimensions, leading to local deformation patterns or distortions in the cross-section under load.
- Medium-Length Columns: These may exhibit coupled (combined) modes of buckling. In these bars, the length is such that both local and global buckling modes can interact, resulting in complex deformation patterns.
- Long Columns: Characterized by global buckling. These are bars with a length that is significantly greater than their cross-sectional dimensions, leading to overall bending or buckling of the entire column.

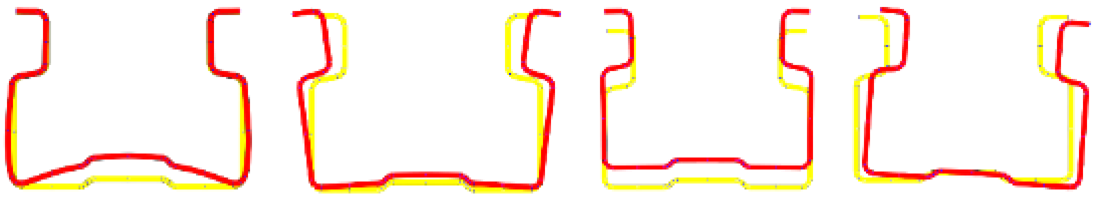

(a) local(L) (b) distortional D) (c) gobal buckling (Í) (d)torsional buckling (R)

Figure 3.16. Typical buckling modes for omga shape columns.

Local buckling occurs through deformation of the front web of the profile (referred to as the web of the profile), and this deformation happens without rotation of the cross-section (Fig. 3.16a).

Distortional buckling occurs on the open side of the profile, through the opening (or closing) of the profile's flanges (Fig. 3.16b).

For long columns, general instability occurs through bending or bending-twisting (Figs. 3.16c and 3.16d).
In the case of thin-walled bars, instability through local wall buckling occurs before the onset of plastic deformation of the section, at point L (Fig. 3.17). Local wall buckling causes a premature loss of rigidity of the bar without leading to its failure. Plastic deformation begins at point B (Fig. 3.17), at the corners of the cross-section, shortly before the failure of the element, at which point section buckling transforms into a local plastic mechanism, concurrently with the onset of general buckling (Dubină et al., 2010). In this scenario, the ultimate load capacity of the bar is lower than that of a bar where no local buckling occurs. Practically, section buckling precedes general buckling, and in design practice, reduced geometric characteristics of the cross-section are used (Dubină, 2000).

3.5. Current research on omega-section columns under compression

Currently, various cross-sectional profiles are utilized in the industry, including thin-walled sections with closed or open (Omega, Sigma, C) contours, as well as symmetrical and asymmetrical sections. The global use of steel pallet racking systems necessitates designing them to ensure structural safety, long-term reliability under diverse environmental conditions and dynamic loads. Recent research has focused on the local, distortional, and global stability of columns, the evaluation of the rigidity of connections between beams and columns, and the lateral stability of beams under bending.
Omega-section perforated columns are used in steel storage structures and are commonly referred to in practice as vertical columns or uprights. These columns feature frontal perforations for the rapid connection of beams and lateral holes for bolt connections. Chapter 7 provides a detailed analysis of the local stability loss of these columns.

3.6 Conclusions

The existing literature contains limited publications on the behavior of beam-column connections under bending tests used in pallet racking systems and the effects of geometric parameters on rigidity and design moment capacity. Recent studies (Zhao et al., 2014; Mohan et al., 2015) indicate that the beam section width and the type of connector affect the connection's rigidity and failure modes, with common failures including rupture and deformation of column profiles and pin cracking or shearing.
Chapter 5 of this thesis examines the effects of column cross-sectional shapes on connection rigidity. Comparative studies on the effects of geometric imperfections imposed in Finite Element Analysis (FEA) of the critical buckling strength, as specified by the European standard EN 1993-1-5, are lacking for short, thin, cold-formed columns under axial loads. Additionally, experimental results on the critical buckling strength and effective section area of thin-profile columns, determined through compression tests for perforated Omega columns used in storage systems, are not available.
The experimental method for determining the effective area of perforated columns according to the EN 15512 (2020) standard is costly and inaccessible for small and medium-sized enterprises. The method for investigating play, specifically the rotation of the connector until the play is eliminated, and its effects on beam deformations and bending moments, are presented in the EN 15512 (2020) standard. Experimental research on the connector rotation angle until play is eliminated could significantly enhance the literature on testing connection elements in metal structures (Schabowicz, 2021).

4. PURPOSE AND OBJECTIVES OF THE DOCTORAL THESIS

The doctoral thesis addresses a topic related to the simulation and testing of components within thin-walled metallic structures, specifically for pallet racking systems. The aim and objectives of the thesis were established considering current solutions for constructing metal structures intended for storage, the practical requirements that such structures must meet (presented in Chapter 1), and the issues and gaps identified in the literature, following the author's review of the current state regarding the calculation, modeling, and mechanical testing of such metal structure components (presented in Chapter 3).

The main objective of the research presented in this thesis is to conduct mechanical testing of the components (beam-to-column connections, support columns) of metal storage structures with pallet racking, as well as to perform numerical simulations of the mechanical behavior of these components. This aims to determine their mechanical properties, identify the main design factors influencing their rigidity and load-bearing capacity, and develop finite element models that simulate the local buckling of columns (uprights), validated by experimental results.

To achieve the main objective mentioned above, the following specific objectives were established for the doctoral thesis:

- Conduct mechanical bending tests on beam-to-column connections using metal connectors with pins, for various combinations regarding beam section sizes, column wall thicknesses, and types of pin connectors (different numbers of pins).
- Determine the rotational rigidities and limit buckling moments for beam-to-column connections in accordance with current standards, for all types of beam-connector-column assemblies involved in the research.
- Study the effects of the type of metal pin connector and the dimensions of the assembled elements (beams and columns) on rotational rigidity and buckling moment recorded at the failure of these connections.
- Investigate the failure modes of beam-to-column connections depending on the connector type, beam section sizes, and column profile wall thickness.
- Incorporate experimental results into a theoretical study on the effects of rotational rigidity of beam-to-column connections on the mechanical behavior of beams with such end connections. This includes evaluating the buckling moment that develops at the end of the beam (at the connection) and the maximum deflection of the beam, for theoretical estimation of safety factors regarding both the connection’s load-bearing capacity and the beam’s rigidity.
- Conduct a comparative theoretical study on the maximum deflection and maximum moment occurring at the mid-span of beams with semi-rigid connections at both ends (as involved in this thesis) versus cases of beams with double-pin or double-fixed ends.
- Conduct mechanical tests to determine the rotation angle of the connection until play is eliminated for different beam-to-connector-to-column assemblies, varying in terms of the thickness of the open-profile section used for the columns.
- Identify the influence of profile wall thickness on the rotation of the connection until play is eliminated in the beam-to-column connector connection.
- Consider experimental results obtained for rotation angles until play elimination in a comparative theoretical analysis of the mechanical behavior of beams with connections at both

ends (as studied), estimating the effects of play in the beam-to-column connections on the bending moment developed at mid-span and the maximum deflection of the beam.

- Conduct mechanical tests to analyze local and distortional buckling of columns made from various perforated profiles with an Omega-shaped open section and thin walls, used in the construction of columns for metal storage structures with pallet racks.
- Determine the critical buckling force and effective area corresponding to the section of profiles used for storage columns, by processing experimental data obtained from mechanical tests on local and distortional buckling.
- Develop finite element models for various perforated profiles with thin walls and an Omega-shaped cross-section used for storage columns, to simulate local and distortional buckling, considering multiple cases of imposed imperfections.
- Conduct a comparative study on the critical buckling force obtained through numerical simulation for various cases considering the size of imposed imperfections in finite element analysis, regarding local and distortional buckling of the columns involved in the research.
- Validate the proposed numerical model for finite element analysis of local and distortional buckling of perforated profiles with an Omega-shaped cross-section by comparing critical buckling forces obtained through numerical simulation with experimental values for all studied profiles.
- Identify the most suitable method for the size of imposed imperfections in the numerical model that reduces errors between numerical and experimental results regarding the critical buckling force for local and distortional instability of the profiles involved in the research.
- Perform a comparative analysis of buckling modes (local or distortional) obtained through numerical simulation with those observed in experimental testing for perforated profiles with thin walls involved in the study.

5. RESEARCH ON THE EFFECTS OF CONSTRUCTIVE PARAMETERS ON THE RIGIDITY OF BEAM-TO-COLUMN CONNECTIONS IN STORAGE SYSTEMS

5.1 Introduction

The purpose of the research in this chapter is to analyze the impact of the type of metal connector and the dimensions of the elements (beams and columns) on the rotational rigidity and bending moment of connections in pallet rack storage systems. The objectives include: (i) testing beam-connector-column assemblies with four or five-pin connectors; (ii) comparing the rigidity of connections based on the type of connector; (iii) analyzing the effects of column wall thickness and beam cross-section dimensions on rigidity and moment capacity; (iv) comparing safety coefficients for different connections to identify the best option; (v) comparing the maximum deflections estimated for beams with semi-rigid connections at both ends. Experimental results for rotational rigidity and bending moments are used to evaluate the maximum deflections of the beams and compare them with those of beams with joints or rigid connectors.

Eighteen different groups of beam-connector-column assemblies were tested, including three types of beams, three types of column profiles, and two types of connectors, with a total of 101 bending tests performed.

5.2 Tested connections

The main elements used in the beam-to-column connections in the pallet rack storage structure industry are shown in Figure 5.1.

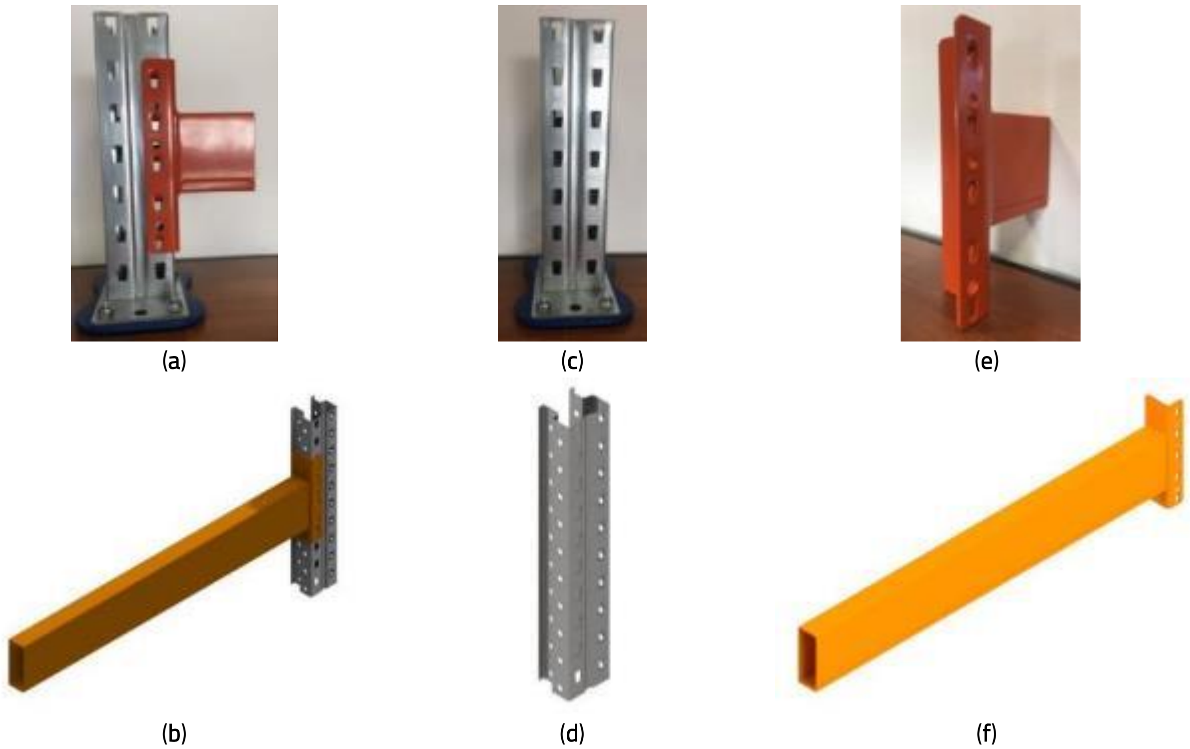

Figure 5.1. The main elements used in the experimental tests are: (a, b) beam-connector-column assembly; (c, d) column; (e, f) beam with welded connector (Dumbrava and Cerbu, 2020a).

The upright shown in Figure 5.1(c) and Figure 5.1(d) is a thin-walled profile obtained by cold rolling. The cross-sectional shape is similar to the omega letter shape (Fig. 5.2). The upright has perforations along its entire length, which allow for the connection with the load-bearing beams through the metal pins present on the surface of the metal connector. The main dimensions for the upright sections used in this research are presented in Table 5.1.
The beams have a rectangular cross-section with thin walls (Fig. 5.1e and Fig. 5.1f) and are made from two assembled C profiles (Fig. 5.3). The main dimensions of the beams used in the research presented in this chapter are given in Table 5.2.

Table 5.1. The dimensions of the cross-sections of the uprights used (Dumbrava and Cerbu, 2020a).

Type of the Upright	Code of the Upright	D* (mm)	W* (mm)	b* (mm)	t* (mm)
90x1.50	I				1.50
90x1.75	II	70	90	50	1.75
90x2.00	III				2.00

**Dimensions of the uprights are shown in Figure 5.2.*

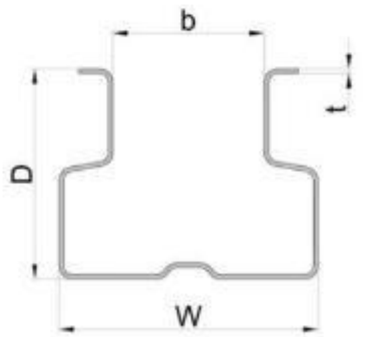

Figure 5.2. The shape and dimensions of the cross-section of the uprights (dimensions D, W, B, t are provided in Table 5.1) (Dumbrava and Cerbu, 2020).

Table 5.2. The dimensions of the cross-sections of the beams used (Dumbrava and Cerbu, 2020a).

Beam Type	Beam Code	H* (mm)	W* (mm)	t* (mm)
BOX 90	A	90	40	1.50
BOX 100	B	100	40	1.50
BOX 110	C	110	40	1.50

** Dimensions of the beams are shown in Figure 5.3.*

Figure 5.3. The shape and dimensions of the cross-sections of the beams (dimensions D, W, b, t are given in Table 5.2) (Dumbrava and Cerbu, 2020a).

Table 5.3 presents the general dimensions (Figure 5.4) and the corresponding codes for each type of connector used in this experimental study.

Table 5.3. Dimensions of the metal pin connectors (Dumbrava and Cerbu, 2020a).

Connector Type	Connector Code	No. Of Tabs	H (mm)	D (mm)	W (mm)	Thickness (mm)
Conector with 5 Tabs	5L	5	238	63	41	4.0
Connector with 4 Tabs	4L	4	190	63	41	4.0

* *Dimensions of the connectors are shown in* figure 5.4.

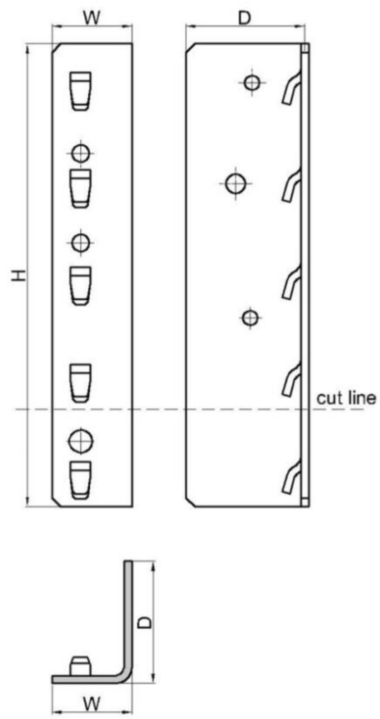

Figure 5.4. The shape and dimensions of the metal pin connectors used in this experimental study (dimensions are given in Table 5.3) (Dumbrava and Cerbu, 2020a).

Table 5.4. The beam-upright-connector assemblies that were tested (Dumbrava and Cerbu, 2020a).

Assembly Identification Code	Upright	Beam	Connector Type	Number of Tests for Assembly
A-I-4L	90x1,50	A (BOX 90)	4L	5
A-I-5L			5L	6
A-II-4L	90x1,75		4L	6
A-II-5L			5L	6
A-III-4L	90x2,00		4L	6
A-III-5L			5L	6
B-I-4L	90x1,50	B (BOX 100)	4L	5
B-I-5L			5L	6
B-II-4L	90x1,75		4L	6
B-II-5L			5L	6
B-III-4L	90x2,00		4L	3
B-III-5L			5L	5
C-I-4L	90x1,50	C (BOX 110)	4L	6
C-I-5L			5L	6
C-II-4L	90x1,75		4L	6
C-II-5L			5L	6
C-III-4L	90x2,00		4L	5
C-III-5L			5L	6

Table 5.4 presents the combinations used in the experimental study to determine the rotational stiffness and the capable bending moment of the tested assemblies, including the identification codes. The three types of uprights tested have the same cross-sectional shape, differing only in profile thickness: 1.50 mm, 1.75 mm, and 2.00 mm. Each beam and upright combination was tested with two types of connectors: with four or five metal pins. In total, 101 individual tests were conducted for all beam-upright-connector combinations. The tested materials were provided by SC Dexion Storage Solutions SRL (Râșnov, Romania).

5.3. Testing methods used to determine the rotational stiffness of beam-upright connections

5.3.1. Tensile testing for steel

For each component of the tested assembly (upright, connector, beam) used in this experimental study, samples were taken to determine the material characteristics. All elements are made of steel, and therefore, tensile tests were performed according to the European standard EN15512 (2020). The tensile tests provided the actual material properties of the steel components, including yield strength, ultimate tensile strength, and elongation at maximum force. These material characteristics obtained from tensile testing are then used in the analysis of the experimental data.

The samples for these tests were cut from the tested components (upright, connector, beam) as shown in Figure 5.5.

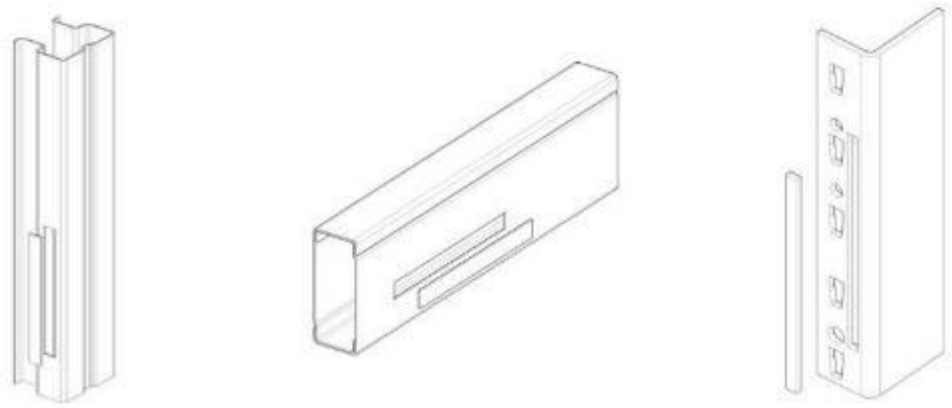

(a) (b) (c)

Figure 5.5. The areas from which the samples for the tensile tests were taken: (a) from the upright; (b) from the beam; (c) from the connector (Dumbrava and Cerbu, 2020a).

5.3.2. Bending tests for upright-connector-beam assemblies

The bending tests for the beam-connector-upright assemblies were conducted according to the EN 15512 (2020) standard. The loading scheme used for the bending tests of the connections, as well as the photograph of the testing rig, are shown in Figure 5.6. It is noted that this specialized bending test rig (Fig. 5.6b), used for all the tests whose results are presented in this chapter, is located in the Mechanical Testing Laboratory at SC Dexion Storage Solutions SRL (Râșnov, Romania). The author of the doctoral thesis played a crucial role in designing and constructing this experimental rig while being employed by this company. SC Dexion Storage Solutions SRL is directly interested in the results of the research presented in this chapter.

According to Figure 5.6(a) and the European standard EN 15512 (2020), a short upright was attached to a very rigid test frame at two points 470 mm apart. A beam, 650 mm long, was connected to the upright using the connector. Lateral movement and twisting of the beam were prevented. The beam was able to move freely in the vertical direction of the load because a steel plate welded to the free end of the beam was guided between bearings. The vertical force was applied at a distance of 400 mm from the upright (Fig. 5.6a), using a SEG Instruments force transducer with an accuracy of 0.001 kN and a maximum capacity of 12.5 kN.

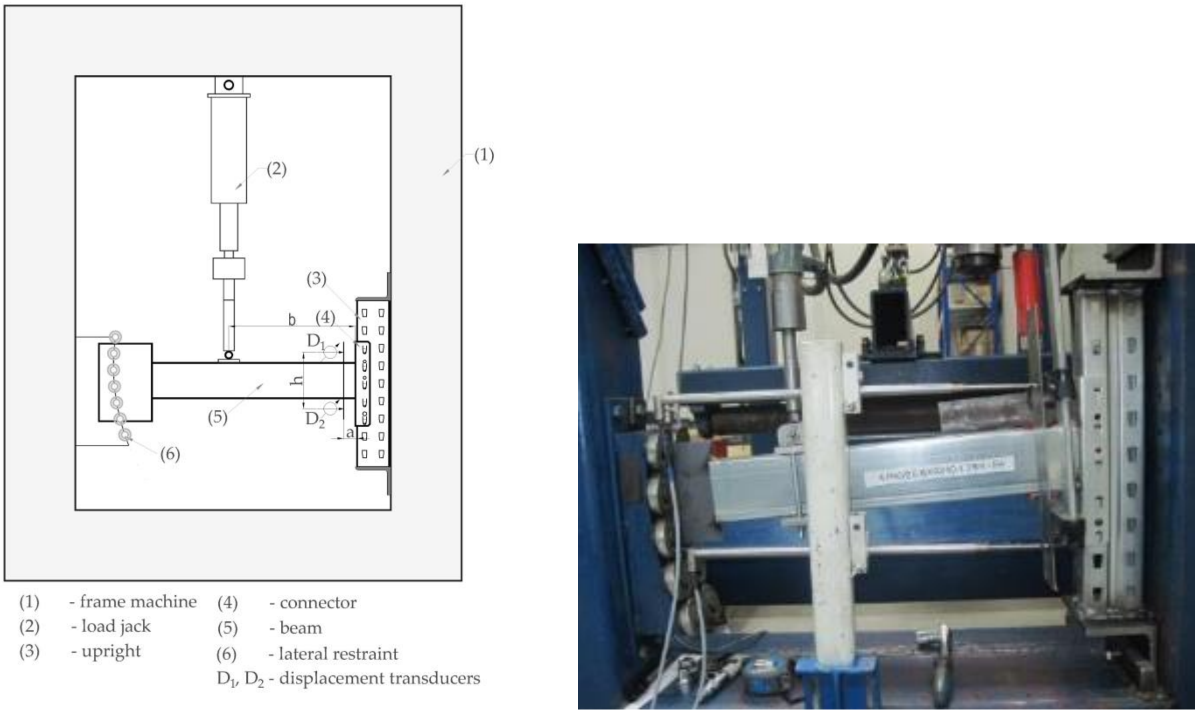

(a) (b)

Figure 5.6 Bending test according to EN 15512 (2020): (a) Loading scheme; (b) Photograph of the experimental rig (Dumbrava and Cerbu, 2020a; Dumbrava and Cerbu, 2022a).

The rotation of the connection was measured using displacement transducers whose probes are in constant contact with the plate fixed to the beam, close to the connector, so that the distance a equals 50 mm (see Fig. 5.6a). The WA-100 displacement transducers (manufactured by HBM - Hottinger Baldwin Messtechnik) can record displacements with a range of less than 100 mm and have a precision of 0.001 mm.

The tests were repeated identically for each beam-connector-upright assembly listed in Table 5.4. A minimum of three tests were conducted for each type of beam-connector-upright assembly shown in Table 5.4, allowing for analysis of the variability in the results.

5.4 Experimental results and discussions

5.4.1. Results from steel tensile tests

Table 5.5 presents the tensile properties of the materials from the tensile specimens taken from each type of component in the beam-upright-connector assembly. The tensile test results for the steel corresponding to the four-pin connectors are identical to those for the five-pin connectors, as five-pin connectors were used for all beams, and the four-pin connectors were obtained by cutting down the five-pin connectors. This approach was chosen to ensure that the same material was used for both types of connectors.

Table 5.5. Material properties of the components tested in the beam-connector-upright assembly (Dumbrava and Cerbu, 2020a).

Component Coresponding to the Tensile Specimen	Measured Thickness	Yield STress $(Rp,02)$ σ_c^*	Ultimate Stress σ_l^*	Elongation
	(mm)	(MPa)	(MPa)	(%)
Upright I (90 × 1.50)	1.48	447.9	528.9	19.2
Upright II (90 × 1.75)	1.80	496.2	536.2	15.3
Upright III (90 × 2.00)	2.09	535.1	590.2	18.5
Beam A (box 90)	1.25	360.6	459.5	38.8
Beam B (box 100)	1.23	379.8	429.5	29.7
Beam C (box 110)	1.27	344.2	411.6	38.1
4-tab connector Box 90	4.04	409.9	469.8	25.6
5-tab connector Box 90	4.04	409.	469.8	25.6
4-tab connector Box 100	4.07	395.3	464	32.6
5-tab connector Box 100	4.07	395.3	464	32.6
4-tab connector Box 110	4.05	444.7	503.5	24.5
5-tab connector Box 110	4.05	444.7	503.5	24.5

* Aceste valori au fost obținute prin încercări de tracțiune, realizate pe mașina de testare INSTRON 3369.

5.4.2. Results from bending tests

All the beam-connector-upright assemblies listed in Table 5.4 were tested according to the procedure outlined in the European standard EN 15512 (2020).

To compare the effects of connector type on the bending behavior of beam-connector-upright connections, the average moment-rotation curves (θ-M) are analyzed. These curves are illustrated in Figures 5.8, 5.9, and 5.10 for each set of assemblies containing beam types A, B, and C, respectively. The results reveal the nonlinear behavior of the connections and show that assemblies with five-pin connectors consistently provide higher rotational stiffness compared to those with four-pin connectors across all tested assemblies, which was anticipated.

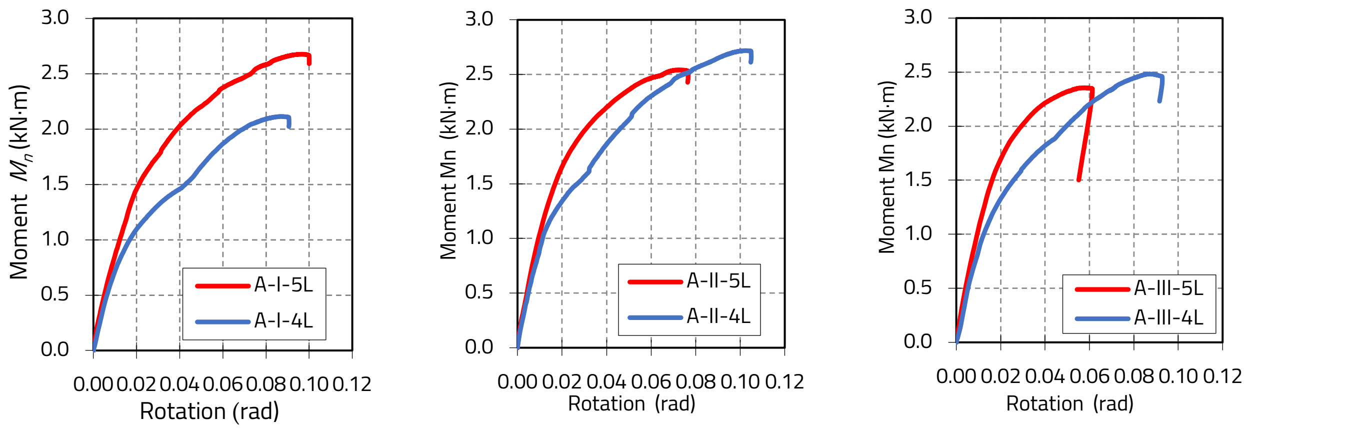

(a) (b) (c)

Figure 5.8. Comparison of the oment-Rotation Curves determined for assemblies: (a) A-I-4L vs. A-I-5L; (b) A-II-4L vs. A-II-5L; (c) A-III-4L vs. A-III-5L (Dumbrava and Cerbu, 2020a).

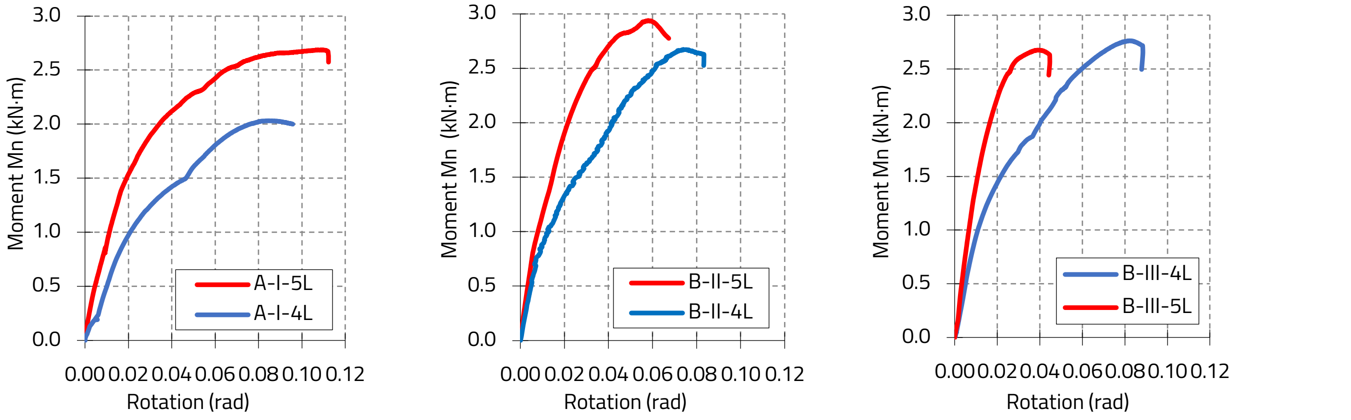

(a) (b) (c)

Figure 5.9. Comparison of the Moment-Rotation Curves determined for assemblies: (a) B-I-4L vs. B-I-5L; (b) B-II-4L vs. B-II-5L; (c) B-III-4L vs. B-III-5L (Dumbrava and Cerbu, 2020a).

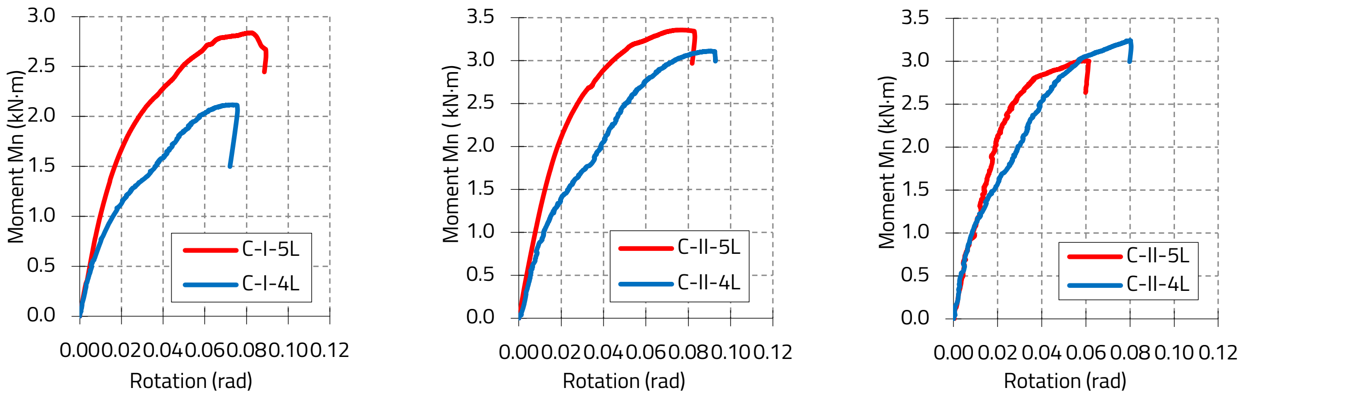

(a) (b) (c)

Figure 5.10. Comparison of the Moment-Rotation Curves determined for assemblies: (a) C-I-4L vs. C-I-5L; (b) C-II-4L vs. C-II-5L; (c) C-III-4L vs. C-III-5L (Dumbrava and Cerbu, 2020a).

To perform the comparative analysis of the test results, the rotational stiffness k_{ni} of the connection for a given assembly type was determined at the maximum bending moment, when the moment capacity M_{Rd} equals 1. All the obtained results are presented in Table 5.6.

The table also provides the average values and standard deviations for both the bending moment capacity M_{Rd} and the rotational stiffness k_m corresponding to each beam-connector-upright assembly group subjected to bending. The ratio of the standard deviation to the average value for the bending moment capacity M_{Rd} across each tested assembly group is, on average, 0.0362 (or 3.62%), indicating a high level of accuracy in the experimental tests.

Similar observations can be made regarding the ratios of the standard deviations to the average values for the rotational stiffness k_m of each tested assembly.

Table 5.6. Bending test results for all studies assemblies (Dumbrava and Cerbu, 2020a).

Assembly code	Design Moment			Rotational Stiffness		
	M_{ni} (kNm)	M_{Rd} (kNm)	Stdev (kNm)	k_{ni} (kNm/ rad)	k_m (kNm/ rad)	Stdev (kNm/ rad)
A-I-4L	2.11	1.54	0.12	40	39.0	1.34
	1.99			38		
	2.08			38		
	1.90			37		
	1.81			40		
A-I-5L	2.68	2.3	0.07	47	48.0	6.18
	2.65			45		
	2.77			48		
	2.60			40		
	2.78			55		
	2.64			56		
A-II-4L	2.73	2.43	0.05	41	42.0	3.37
	2.75			37		
	2.72			40		
	2.84			45		
	2.77			45		
	2.81			45		

Assembly code	Design Moment			Rotational Stiffness		
	M_{ni} (kNm)	M_{Rd} (kNm)	Stdev (kNm)	k_{ni} (kNm / rad)	k_m (kNm / rad)	Stdev (kNm / rad)
B-I-4L	2.03	1.84	0.02	34	35.9	1.38
	2.06			36		
	2.08			35		
	2.07			38		
	2.07			37		
B-I-5L	2.69	2.24	0.12	55	57.8	7.29
	2.75			59		
	2.62			46		
	2.58			61		
	2.76			58		
	2.92			68		
B-II-4L	3.04	2.03	0.18	56.1	56.0	1.65
	2.67			54.3		
	2.87			57.6		

Assembly code	Design Moment			Rotational Stiffness		
	M_{ni} (kNm)	M_{Rd} (kNm)	Stdev (kNm)	k_{ni} (kNm / rad)	k_m (kNm / rad)	Stdev (kNm / rad)
C-I-4L	2.12	1.70	0.08	44	43.7	1.26
	2.13			44		
	2.13			45		
	1.95			41		
	2.14			44		
	1.96			40		
C-I-5L	2.84	2.15	0.20	72	77.4	5.71
	3.05			73		
	3.01			73		
	2.60			80		
	2.61			81		
	2.69			86		
C-II-4L	3.08	2.74	0.03	50.1	52.4	2.97
	3.03			49.3		
	3.07			52.8		
	3.11			53.1		
	3.08			56.8		

A-II-5L	2.54	2.21	0.09	63	76.0	13.5	B-II-5L	2.66	2.36	0.10	65	86.1	15.7	C-II-5L	3.29	2.95	0.06	79	83.7	7.25
	2.69			57				2.78			77				3.39			93		
	2.79			74				2.75			76				3.36			81		
	2.60			81				2.85			100				3.35			80		
	2.59			91				2.87			105				3.47			93		
	2.57			88				2.94			94				3.35			77		
A-III-4L	2.57	2.16	0.06	41	45.0	3.57	B-III-4L	2.76	2.43	0.03	50	51.2	2.97	C-III-4L	3.28	2.89	0.03	63	63.0	2.93
	2.48			43				2.74			50				3.27			67		
	2.40			42				2.78			47				3.24			64		
	2.49			44				2.75			53				3.20			64		
	2.50			48				2.70			55				3.27			61		
	2.52			50				2.71			52				3.24			58		
A-III-5L	2.36	2.09	0.02	73	77.0	8.90	B-III-5L	2.52	2.18	0.07	80	102	20.9	C-III-5L	2.92	2.61	0.06	107	115	9.76
	2.34			65				2.49			86				3.01			101		
	2.34			72				2.55			98				2.99			116		
	2.34			81				2.55			114				2.94			121		
	2.31			84				2.68			131				3.00			119		
	2.37			89											3.08			128		

The analysis of the low values recorded for the standard deviation (denoted as stdev) compared to the average rotational stiffness k_m shows that the degree of dispersion in the results is minimal. The differences between the results obtained for assemblies within the same set are attributed to the geometric imperfections of the cross-sections, which are characteristic of cold-formed steel profiles.

5.5 Failure modes of beam-column connections in bending tests

In the bending tests, the failure mode varied from one assembly to another. Column failure is the primary failure mode, especially for assemblies where the column profile thickness was 1.50 mm (see Fig. 5.14). This occurs because when the beam is loaded and the connector rotates, the first two pins are subjected to the greatest stress, causing deformation of the column in the perforation areas, as the beam experiences tensile normal stresses in the upper part (see Fig. 5.14c).

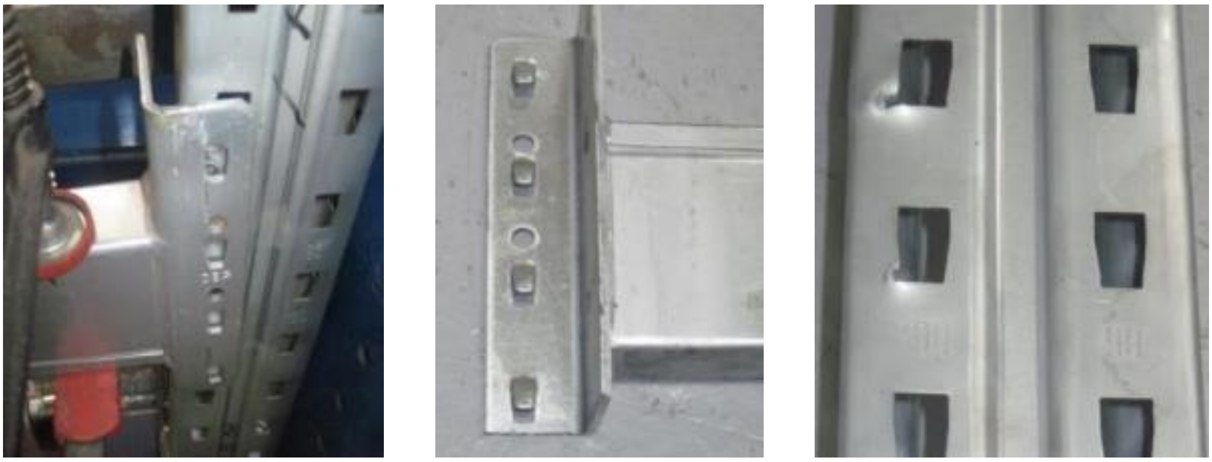

(a) (b) (c)

Figure 5.14. Failure modes for columns with a wall thickness of 1.50 mm: (a, b) failure modes for the connector; (c) failure mode in the perforation area on the front side of the column (Dumbrava and Cerbu, 2020a).

(a) (b) (c)

Figure 5.15. Modes of Failure in Assemblies Containing Columns with a Wall Thickness of 1.75 mm: (a) Mode of failure of the metallic pin connector; (b) Mode of failure of the beam; (c) Mode of failure of the column (Dumbrava and Cerbu, 2020a)

It was observed that as the thickness of the column increases, the failure mode changes for columns with a thickness of 1.75 mm. All components (the column, connector, and beam) begin to be part of the failure mode (Fig. 5.15). In this case, rotation decreases (Fig. 5.15a), especially if the height of the beam section increases. The lower part of the beam is subjected to normal compressive stresses and starts to buckle locally (Fig. 5.15b). The connector also deforms under the bending load (Fig. 5.15a).
In assemblies with columns having a profile thickness of 2.00 mm, the effects of the metal pins in the connector on the column are very minimal, especially for the five-pin connector (fig. 5.16a, fig. 5.16c). It is observed that the rotation of the connector is smaller (fig. 5.16a), indicating that the highest rotational stiffness corresponds to these situations (see Table 5.6). In this case, the primary failure modes are the bending of the connector (fig. 5.16a) and local deformation of the beam near the connector (fig. 5.16b). For the assembly with the four-pin connector (fig. 5.17), due to the greater rotation of the beam compared to the assembly with the five-pin connector, the top pin deforms the column in the slot where the metal pin is mounted (fig. 5.17c).

(a) (b) (c)

Figure 5.16. Failure modes in assemblies with columns having a wall thickness of 2.00 mm and five-pin connectors: (a) failure mode of the connector; (b) failure mode of the beam; (c) failure mode of the column (deformation of the slot shape) (Dumbrava and Cerbu, 2020a).

(a) (b) (c)

Figure 5.17. Failure modes in assemblies with columns having a wall thickness of 2.00 mm and four-pin connectors: (a) failure mode of the connector; (b) failure mode of the beam; (c) failure mode of the column, slot deformation (Dumbrava and Cerbu, 2020a).

5.6 Effects of connection rotation rigidity between beam and column on beam mechanical behavior

The experimental values obtained for the design moment M_{Rd} and rotation rigidity k_m of the connection are crucial for verifying the safety of the beam-connector-column assembly, from both a strength and rigidity perspective. In a typical example for pallet racking systems, two beams, each 2.7 meters long, must support the weight of three wooden pallets, each weighing 500 kg. The total weight of the three pallets is 15,000 N, distributed evenly across the two beams, resulting in a force of 7,500 N per beam, or a uniformly distributed load of 2.78 N/mm. It is assumed that these beams are connected to the columns via semi-rigid connections, with the values of M_{Rd} and k_m specified in Table 5.6.

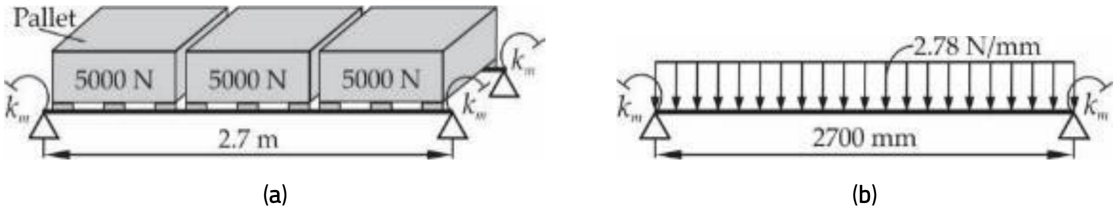

Figure 5.18. Loading Diagram for the Pallet Storage System Rack: (a) Loading on two beams to support three pallets; (b) Equivalent loading diagram for a single beam, incorporating the rotational stiffness k_m of the beam-to-column connection (Dumbrava and Cerbu, 2020a)

To better understand the importance of experimentally determining the rotational stiffness of the beam-to-column connection, a comparative study is presented for the same practical case previously discussed, corresponding to beam type B for the following different situations regarding the rotational stiffness of the beam end connections:

- Beam Type B, shown in Figure 5.19(a): For which the rotational stiffness of the connections is zero, corresponding to pinned ends of the beam.
- Beam Type B, shown in Figure 5.19(b): For which the rotational stiffness of both end connections is 35.9 kN·m/rad, corresponding to semi-rigid connections.
- Beam Type B, shown in Figure 5.19(c): For which the rotational stiffness of both end connections is 102 kN·m/rad, corresponding to semi-rigid connections.
- Beam Type B, shown in Figure 5.19(d): For which the rotational stiffness of the connections is infinite, corresponding to rigid connections (double fixed beam).

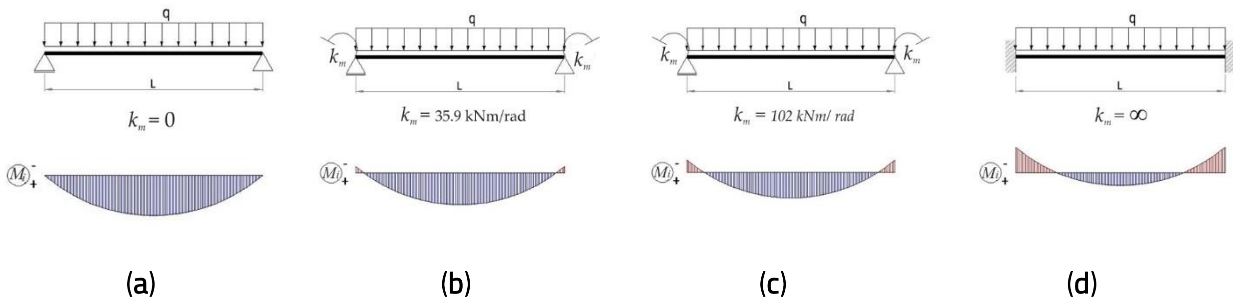

Figure 5.19. The diagrams for the bending moment for all boundary conditions of Beam Type B are as follows: (a) Beam with pinned supports at both ends.; (b) Semi-rigid connection with a four-pin metal connector;(c) Semi-rigid connection with a five-pin metal connector; (d) Rigid connection. Dumbrava and Cerbu, 2020a).

It is noted that all results are presented for cases involving the type B beam assembly. For the numerical models of beams with semi-rigid connections at both ends (Fig. 5.19b, Fig. 5.19c), only cases corresponding to the extreme values of rotational stiffness (the smallest and largest values) are considered.

For visual comparisons, Fig. 5.20 and Fig. 5.21 display the bending moment diagrams and, respectively, the deflection diagrams (vertical displacements) for all cases shown in Fig. 5.19.

The comparison of results presented in Figs. 5.20 and 5.21 highlights the importance of determining the rotational stiffness for such semi-rigid connections, as deflection, bending moments, and stresses are influenced by support conditions.

Comprehensive details on the analysis of these semi-rigid connections can be found in the complete thesis.

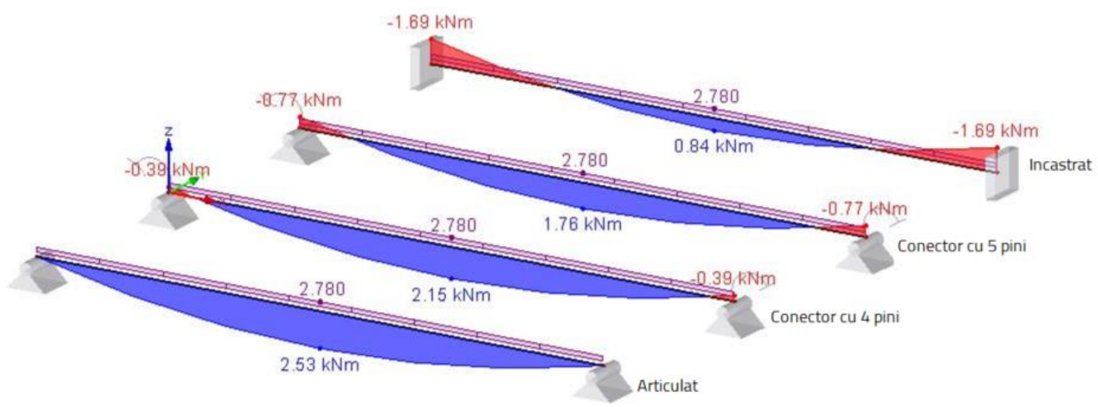

Figure 5.20. Comparison of bending moment diagrams for all support conditions considered for the type B beam (Dumbrava and Cerbu, 2020a).

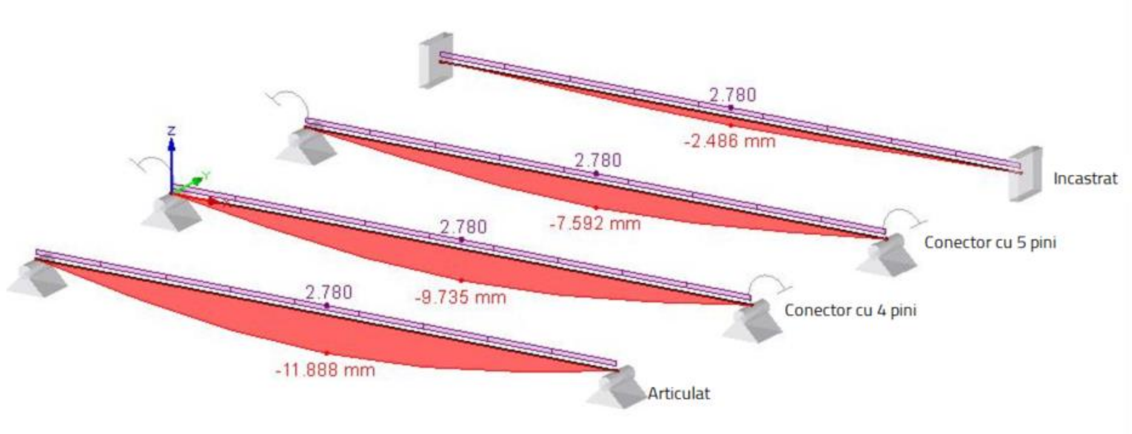

Figure 5.21. Comparison of maximum deflections v_{max} for all support conditions considered for the type B beam (Dumbrava and Cerbu, 2020a).

5.7 Conclusions

Semi-rigid connections are commonly used in the metal storage systems with pallet racks industry. This experimental study investigates the mechanical behavior of the connectors at the ends of beams used for assembling them with columns. The primary objective of the research presented in this chapter was to examine the influence of the connector type (four-pin connector and five-pin connector) and the effects of column profile thickness on the load-bearing capacity of the connections under mechanical loads. For all tested beam-connector-column assemblies, moment-rotation curves were plotted. Additionally, the experimentally obtained values for the design moment M_{Rd} capacity and rotational stiffness k_m of the connections were compared. Complete details about this analysis are presented in the full doctoral thesis.

6. RESEARCH ON THE EFFECTS OF LOOSENESS IN BEAM-COLUMN CONNECTIONS ON SECTIONAL FORCES AND BEAM DEFLECTIONS

6.1. Aspects of looseness in beam-column connections used in metal pallet racking systems

In the design of pallet racking systems, the mechanical behavior of semi-rigid joints is assessed through tests in accordance with the European standard EN 15512. The 2020 version of this standard includes procedures for adjusting bending moments and maximum beam deflections due to clearances between beams and columns. Connections may be bolted or pinned, each with its own advantages and disadvantages: bolted connections are less economical, while pinned connections are faster to install and offer more flexibility. However, pinned connectors require the initial clearances to be considered in the design calculations. The latest version of the EN 15512 standard details the testing method for connector rotation and the effects of clearances on deformations and bending moments, contributing significantly to the field.

In the case of clearances in bolted connections (see Fig. 6.1), the sliding effect can also be observed (see Fig. 6.2). The main difference compared to pinned connections is that, in bolted connections, the sliding effect does not occur at the beginning of the moment-rotation curve (see Fig. 6.2).

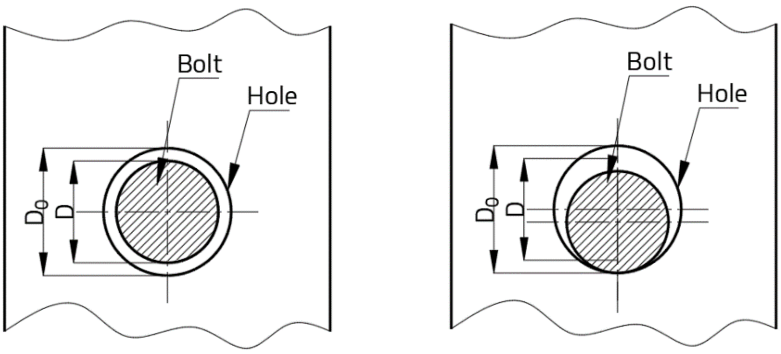

(**a**) (**b**)

Figure 6.1. Looseness in Bolted Connections: (a) Looseness between the bolt and the hole; (b) Actual looseness when the bolt is in contact with the hole (Dumbrava and Cerbu, 2022a).

In contrast to bolted connections, the European standard EN 15512 highlights the need to consider the looseness present in pin connector joints used between columns and beams in the structural analysis of pallet rack storage systems. The effects of looseness in these connections become apparent at lower loads compared to bolted connections. This behavior is explained by the fact that bolts are generally pre-tensioned, whereas pin connectors lack a general rule accounting for the effects of looseness due to varying forms and dimensions of both the column perforations and the pin connectors fixed at the beam ends.

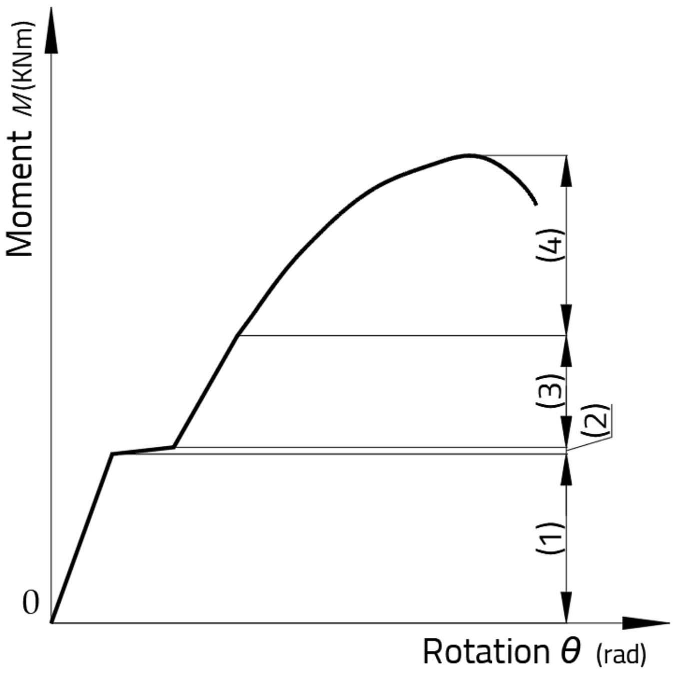

Figure 6.2. Typical behavior of bolted connections in cold-formed steel structures: (1) - linear behavior before slipping (elimination of looseness); (2) - effects of slipping caused by the looseness between the bolt and the hole; (3) - linear behavior after the elimination of looseness; (4) - nonlinear behavior (Dumbrava and Cerbu, 2022a).

6.2. Materials tested and methodology.

6.2.1. Types of tested assemblies

The purpose of the experimental program is to determine the effects of looseness in the pin connector connection between the beam and the column for three different types of connections, as presented in Table 6.1.

The identification codes corresponding to the beam-column-connector assemblies that were tested are presented in Table 6.1 and are used for presenting the results obtained.

Table 6.1. Assemblies of the beam-column-connector type tested (Dumbrava and Cerbu, 2022a)

Assembly code	Upright $W^* \times t^*$	Beam $H^{**} \times W_1^{**} \times t_1^{**}$	Conector type	Number of looseness tests for assembly	Numbar of bending tests for assembly
0-I–5T	90 x 1.50	BOX 150 x 50 x 1.75	5T	4	6
0-II–5T	90 x 1.75			4	6
0-III–5T	90 x 2.00			4	6

*The dimensions of the uprights are shown in Figure 6.3(a).

**The dimensions of the beams are shown in Figure 6.3(b).

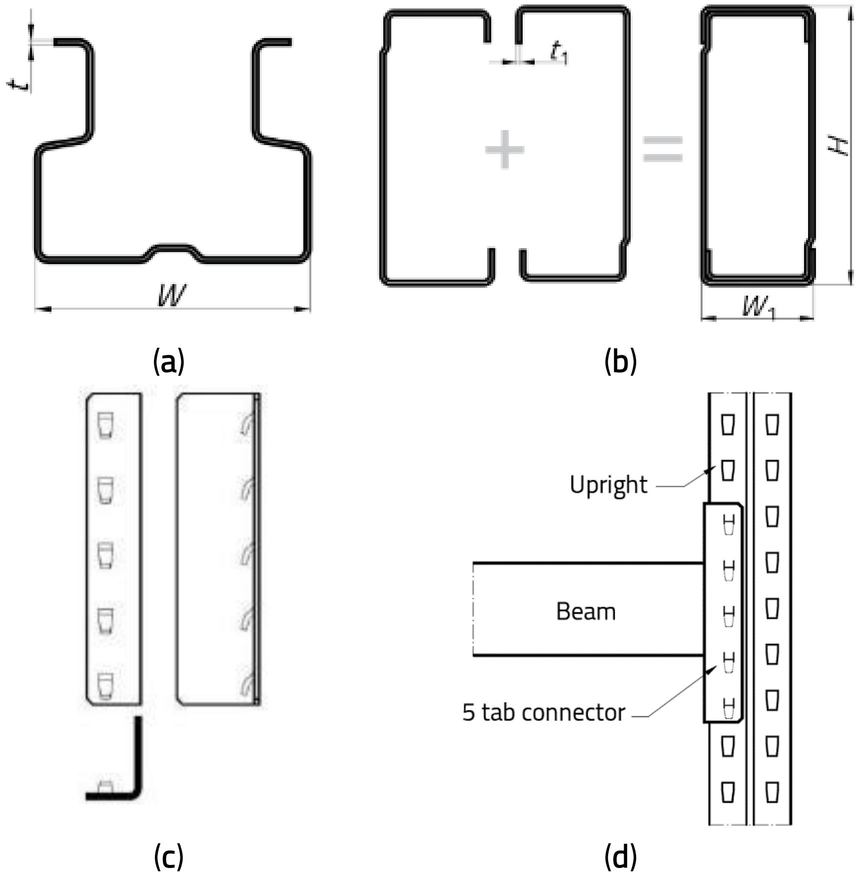

Figure 6.3. Components of the column-connector-beam assemblies: (a) column section; (b) beam section; (c) 5-pin connector; (d) sketch of the tested assembly (Dumbrava and Cerbu, 2022a).

The components of the beam-connector-column assemblies tested are shown in Figure 6.3. Three columns with different cross-sections (Fig. 6.3a) were used, all having the same shape but varying wall thicknesses (1.50 mm, 1.75 mm, and 2.00 mm), as presented in Table 6.1. The same composite beam, created by joining two C profiles (Fig. 6.3b), is connected to the column using a five-pin metal connector (Fig. 6.3c), which is welded to the end of the beam. For each tested assembly (Fig. 6.3d and Table 6.1), the same type of five-pin connector, coded as 5T in Table 6.1, was used. A beam with a high moment of inertia about the principal axis (with greater rigidity) was used to minimize the effect of beam deformations during the mechanical tests aimed at determining the rotation of the connector until the existing clearances in the connection between the beam and columns were eliminated. An example of a tested assembly is shown in Figure 6.3(d). Sets of four individual assemblies were prepared for each testing configuration to determine the effects of existing clearances in the connection (see the penultimate column in Table 6.1), resulting in a total of 12 assemblies for testing. Additionally, a set of six assemblies of each type of beam-connector-column configuration (see the last column in Table 6.1) was prepared for bending tests to determine the rotational rigidity of the respective connection.

6.2.2. Methodology for bending tests to determine the effects of existing clearances in the beam-column connection

The different beam-connector-column assemblies were subjected to bending tests and tests to determine the rotation of the connector until the clearances in the beam-column connection with pin connectors were eliminated, according to the European standard EN 15512 (2020).
The experimental setup is shown in Figure 6.4 and is the same for both the bending test and the test used to determine the effects of clearances in the beam-column connection, in accordance with the European standard EN 15512 (2020). The loading scheme for this experimental stand is identical to that presented in Figure 5.6(a) in Chapter 5. Figure 6.4 shows a photograph of the stand taken during the testing of a beam-connector-column assembly. It is reiterated that this specialized bending test stand, on which all tests whose results are presented in this chapter were conducted, is located in the Mechanical Testing Laboratory of SC Dexion Storage Solutions SRL (Râșnov, Romania). The author of the doctoral thesis designed and built this experimental stand within the company.

Firstly, the bending test for each type of beam-connector-column assembly was performed to determine the design moment, denoted as M_{Rd}, and the rotational rigidity, denoted as k_m. The bending test for the beam-connector-column assembly and the method for determining both the design moment M_{Rd} and the rotational rigidity k_m are described in the previous chapter of this work, in accordance with the European standard EN 15512 (2020). It should be noted that to determine the rotation of the connector, measured until the clearances in the beam-column connection are eliminated, the loading system must allow the application of the loading force in both directions, that is, both upward and downward (Fig. 6.4a), so that the bending moment can be applied in both directions.

Figure 6.4. Testing rig for bending and rotation tests: (a) Testing stand diagram: Picture of the setup used for both the bending test and the test to determine the rotation of the connector until clearances are eliminated, in accordance with the European standard EN 15512 (2020). (b) Photograph of the testing stand: Photograph taken during the testing of a beam-connector-column assembly, showing the actual experimental setup (Dumbrava and Cerbu, 2022a).

For both the bending tests conducted to determine the rotational stiffness of the beam-to-column connection and the tests aimed at determining the rotation of the connector until the clearances are eliminated, it is necessary to plot the moment-rotation curve ($M - \theta$). According to the notations presented in Figure 5.6(a), the bending moment M_i developing at the connector at the end of the beam, as well as the rotation θ of the connector, expressed in radians, are calculated using relation (6.1) and relation (6.2), respectively.

$$M_i = bF, \tag{6.1}$$

$$\theta = (d_1 - d_2)/h. \tag{6.2}$$

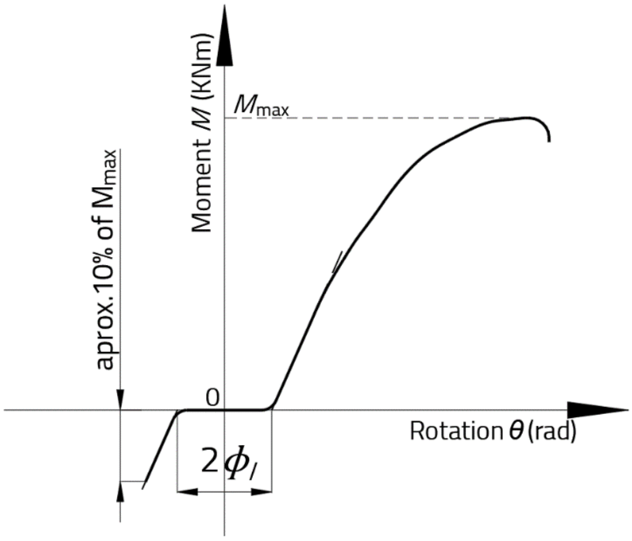

Figure 6.5. Typical moment-rotation curve obtained in the bending test to determine the effects of play in the beam-to-column connection (Dumbrava and Cerbu, 2022a)

In the tests conducted to study the effects of play in the connection, the force F (Fig. 6.4a) was applied gradually until the moment at the connector reached a value approximately equal to 10% of the design moment, denoted by M_{Rd} and calculated using equation (5.12) from Chapter 5. Subsequently, the loading force was reduced and then reversed until the moment value was approximately 10% of the design moment M_{Rd}.

The double of the connector's rotation angle, until the play between the connector pins and the column perforations was eliminated, denoted by $2\Phi_l$, is measured for each test by extrapolating the linear portions of the moment-rotation curve to the origin to find their intersection points with the abscissa (rotation axis), as shown in Fig. 6.5. The difference between the abscissas of these intersection points obtained in this way equals twice the rotation Φ_l of the connector in the beam-to-column connection, corresponding to the moment at which the play was eliminated.

All moment-rotation curves ($M - \theta$) obtained for the beam-connector-column assemblies involved in this research are reported as results. The study also presents the following data obtained from processing the experimental data: the rotation Φ_l of the connector measured at the point of play elimination in the beam-to-column connection, the design moment M_{Rd}, and the rotational stiffness k_m.

6.3. Experimental results

Figure 6.8 shows the moment-rotation curves \(M(\theta) \) recorded in tests conducted to study the effects of play in the beam-to-column connections with pin connectors, for the following beam-connector-column assemblies: 0-I-5L; 0-II-5L; 0-III-5L. These curves were corrected using equations (5.5) and (5.8) from Chapter 5.

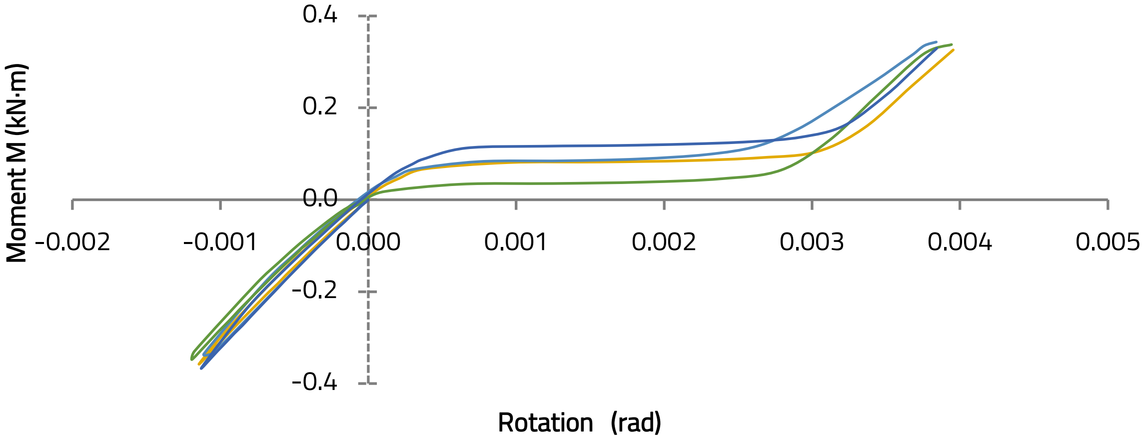

(a)

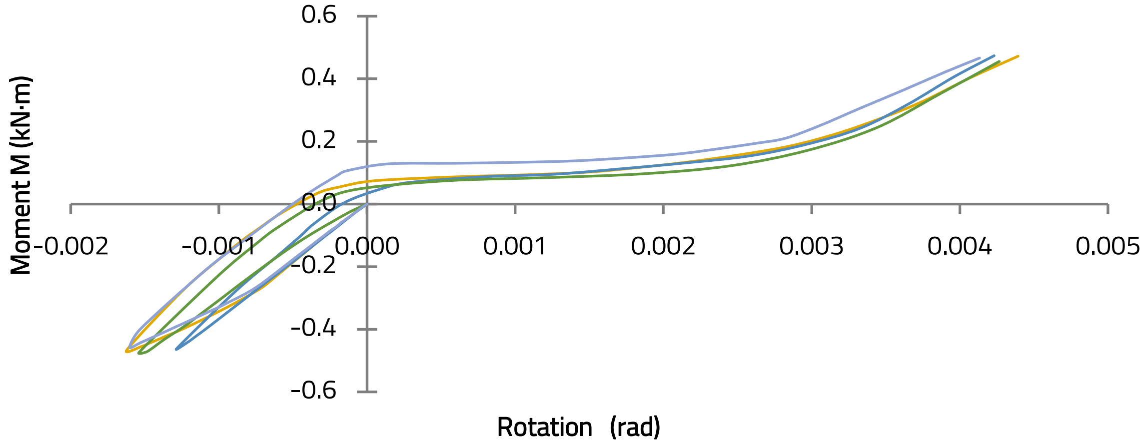

(b)

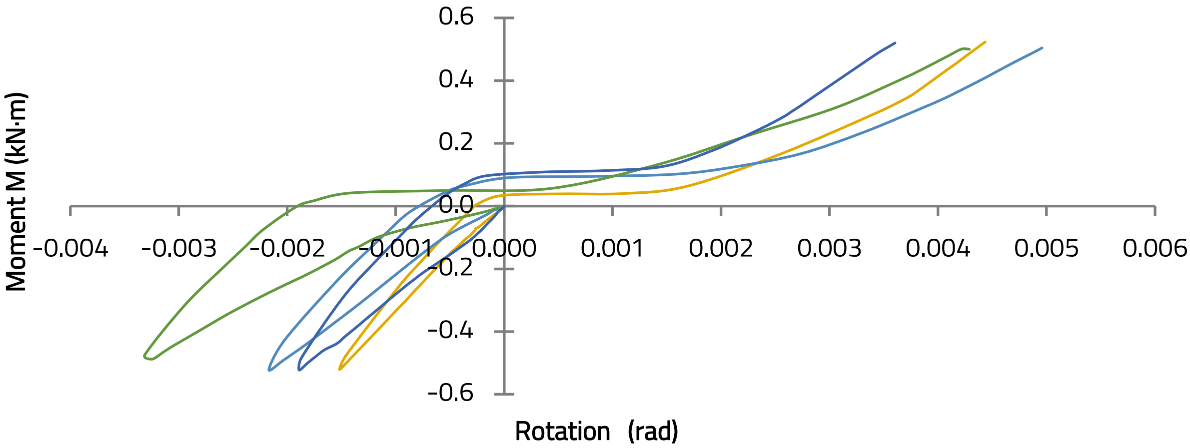

(c)

Figure 6.8. Moment-rotation curve ($M_n - \theta_n$) recorded in the tests conducted to study the effects of looseness in the connections, for the following beam-connector-column assemblies: (a) 0-I-5L; (b) 0-II-5L; (c) 0-III-5L (Dumbrava and Cerbu, 2022a).

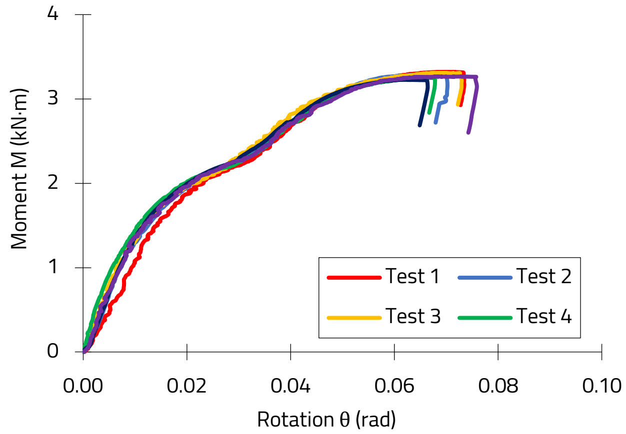

Figure 6.9. Moment-rotation curve $(M_n - \theta_n)$ *recorded in the bending tests for the beam-connector-column assembly of type 0-I-5T (Dumbrava and Cerbu, 2022a).*

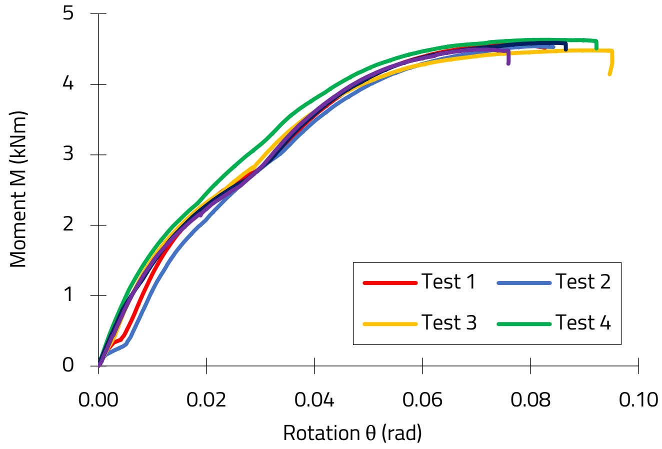

Figure 6.10. Moment-rotation curve $(M_n - \theta_n)$ *recorded in the bending tests for the beam-connector-column assembly of type 0-II–5T (Dumbrava and Cerbu, 2022a).*

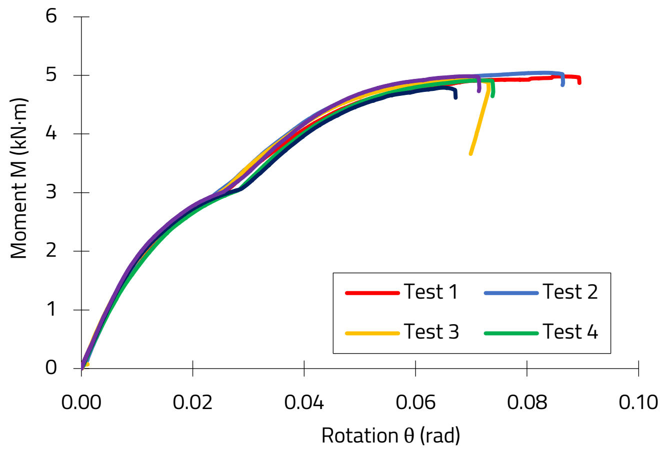

Figure 6.11. Moment-rotation curve $(M_n - \theta_n)$ *recorded in the bending tests for the beam-connector-column assembly of type 0-III–5T (Dumbrava and Cerbu, 2022a).*

The moment-rotation curves (M - θ) recorded in the bending tests for the three investigated beam-connector-column assemblies (0-I-5L, 0-II-5L, and 0-III-5L) are presented in Figures 6.9, 6.10, and 6.11, respectively.

The experimental results regarding the rotation Φ_l of the connector until the clearance is eliminated, the design moment M_{Rd}, and the rotational stiffness k_m for the beam-connector-column assemblies involved in this study are summarized in Table 6.3.

Table 6.3. Results Obtained in Tests for Studying the Effects of Clearances in Beam-Column Connections and in Bending Tests for All Assemblies Involved in the Research (Dumbrava and Cerbu, 2022a)

Assembly code	Looseness angle			Design moment		Rotational stiffness	
	$\Phi_{l\,i}$ (rad)	Φ_l (rad)	Stdev (rad)	M_{Rd} (kN·m)	Stdev (kN·m)	k_m (kN·m/ rad)	Stdev (kN·m/ rad)
0-I-5T	0.00139 0.00140 0.00114 0.00137	0.00133	0.000124	2.91	0.035	72	10.029
0-II-5T	0.00115 0.00126 0.0013 0.00092	0.00116	0.000171	4.02	0.058	96	4.118
0-III-5T	0.00075 0.00093 0.00083 0.00069	0.00080	0.000104	4.32	0.086	114	4.425

6.4. Effects of looseness in beam-column connections

To assess the impact of looseness in pin-connected beam-to-column connections, the maximum deflection v_{max} and bending moment M_{mij} occurring at the midspan of the beam are calculated in the context of pallet rack storage systems. The study is based on the test case presented in Figure 5.18, where the rack consists of two 2.7 m beams supporting a maximum load of 15,000 N (equivalent to three pallets). Assuming each beam carries a uniformly distributed force of 7,500 N over a length of 2.7 m, the force is uniformly distributed at 2.78 N/mm.

The study analyzes the effects of looseness in all types of connections, with rotational stiffness k_m presented in Tables 6.2 and 6.3. The values for the moments of inertia of the beams are taken from the manufacturer's technical documentation. The rotation Φ_l of the connector, at the moment the looseness is eliminated, is considered constant for assemblies combining the same type of column and the same type of connector (4 pins or 5 pins). The research particularly investigated the critical case of connections with 5-pin connectors.

The results regarding rotation Φ_l have been extended and applied to all beam-connector-column assemblies presented in Table 6.2, with specified values in Table 6.4. The calculation of the bending moment M_{mij} and maximum deflection v_{max} was carried out using the appropriate relations, taking into account the effects of looseness in the connections. The obtained results are presented in Table 6.4, compared with those calculated without the effects of looseness.

Table 6.4. Effects of looseness on the bending moment and maximum deflection at the midspan of the beam for the involved column-connector-beam assemblies (Dumbrava and Cerbu, 2022a).

Assembly code	Looseness angle Φ_l (rad)	With looseness effects		Without looseness effects		$CORR_{M_{mid}}$ (%)	$CORR_{v_{max}}$ (%)
		Bending moment at mid. $M_{mid,t}$ (kN·m)	Max. deflection at mid. $v_{max,t}$ (mm)	Bending moment at mid. M_{mid} (kN·m)	Max. deflection at mid. v_{max} (mm)		
0-I-5T	0.00133	3.245	2.83	3.163	2.709	2.59	4.47
0-II-5T	0.00116	3.168	2.753	3.076	2.618	2.99	5.16
0-III-5T	0.00080	3.089	2.662	3.016	2.555	2.42	4.19
A-I-4T	0.00133	2.794	12.383	2.758	12.104	1.31	2.31
A-I-5T		2.692	11.831	2.651	11.511	1.55	2.78
A-II-4T	0.00116	2.753	12.153	2.72	11.897	1.21	2.15
A-II-5T		2.441	10.45	2.394	10.085	1.96	3.62
A-III-4T	0.00080	2.709	11.884	2.685	11.7	0.89	1.57
A-III-5T		2.419	10.297	2.387	10.043	1.34	2.53
B-I-4T	0.00133	2.947	10.325	2.911	10.106	1.24	2.17
B-I-5T		2.735	9.429	2.684	9.122	1.90	3.37
B-II-4T	0.00116	2.744	9.455	2.7	9.193	1.63	2.85
B-II-5T		2.522	8.515	2.465	8.174	2.31	4.17
B-III-4T	0.00080	2.774	9.561	2.746	9.39	1.02	1.82
B-III-5T		2.41	8.01	2.368	7.752	1.77	3.33
C-I-4T	0.00133	2.968	8.321	2.923	8.106	1.54	2.65
C-I-5T		2.715	7.478	2.649	7.158	2.49	4.47
C-II-4T	0.00116	2.887	8.043	2.843	7.83	1.55	2.72
C-II-5T		2.668	7.306	2.607	7.012	2.34	4.19
C-III-4T	0.00080	2.79	7.693	2.755	7.524	1.27	2.25
C-III-5T		2.479	6.64	2.426	6.396	2.18	3.81

6.5. Conclusions

This study analyzes the experimental results regarding the rotation of the connector until the elimination of looseness, according to the European standard EN 15512 (2020), for various beam-connector-column assemblies. Additionally, the assessment of the effects of looseness in connections focuses on their impact on the maximum deflection of the beams and the bending moment at the midspan of the beams used in pallet rack systems. Complete details on these aspects are presented in the full doctoral thesis.

The experimental results show that, for the case studied, the maximum corrections for the calculation of the bending moment and maximum deflection are 2.99% and 5.16%, respectively, compared to the situation where the effects of looseness are neglected. The graphical interpretation highlights that these corrections are more significant when the column wall is thinner. Additionally, the ratio between the maximum deflection calculated considering the effects of looseness and the maximum deflection without these effects is higher for the five-pin connector (ranging from 1.025 to 1.052) compared to the four-pin connector (ranging from 1.016 to 1.029).

7. RESEARCH ON THE COMPRESSION OF COLUMNS IN METAL STORAGE STRUCTURES

7.1. Experimental research on local buckling of columns in storage structures

This chapter addresses the research on the loss of stability in short, perforated steel columns with Omega-shaped cross-sections used in pallet storage systems. The main objective is to determine the critical buckling load and effective area for these columns subjected to compressive forces, as well as to analyze the effects of imperfections in finite element models on the accuracy of results compared to experimental data.

The research involves the following stages:

- Determination of the critical buckling loads for the 15 types of short perforated columns.
- Nonlinear analysis using finite element methods of stability loss for the same columns, with initial imperfections of varying magnitudes.
- Comparison of results obtained from numerical simulations with experimental data to validate the numerical model.

7.1.1. Geometry of the tested columns

This section investigates 15 different steel profiles with Omega-shaped cross-sections used in the manufacture of columns for pallet racking storage systems. These profiles, which are used for columns, were subjected to compression tests. The cross-sectional shape, as well as the front view, for each tested profile is shown in Figure 7.1. Each type of profile is coded with a capital letter.

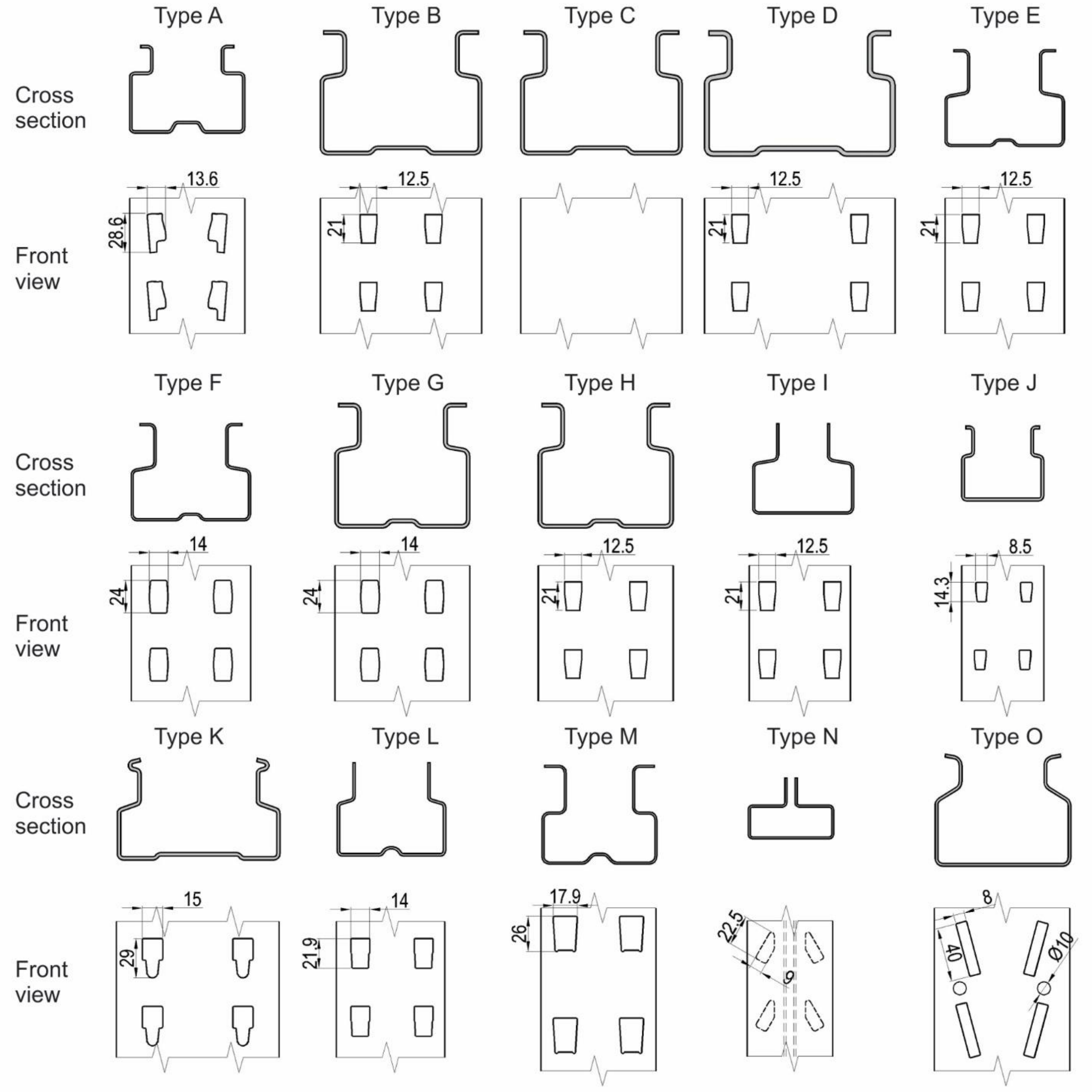

Figure 7.1. The types of columns considered in the study, with different shapes of cross-sections and perforations located on the front side (Dumbrava and Cerbu, 2024)

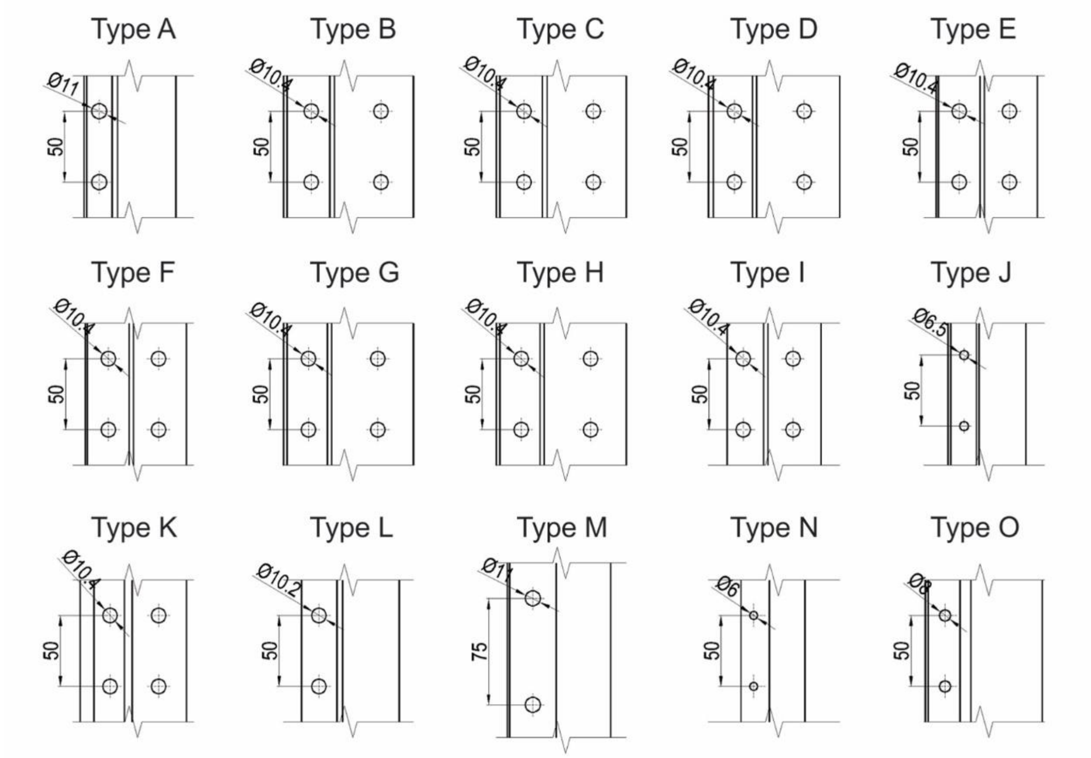

Figure 7.2. The side view of the tested column flanges and their perforations (Dumbrava and Cerbu, 2024).

The notations used for the main dimensions of the cross-section are indicated in Figure 5.2, and the design values for these dimensions are presented in Table 7.1 for all types of columns tested in these studies. The wall thickness of the cross-section was measured for each tested column, as it slightly differs from the nominal thickness due to the manufacturing process, and the corresponding average value is provided in Table 7.1. The side view for each type of tested column is shown in Figure 7.2 to illustrate the dimensions of the perforations located on the flanges.

The specimens for the tensile test were cut from the same steel sheet roll used to create each Omega-shaped profile through cold plastic deformation technologies. The measured thickness of the column and the experimentally obtained yield stress are used in processing the experimental data recorded during the compression test of the profiles, to correct the recorded value of the force at the loss of column stability, in accordance with the European standard EN 15512 (2020).
The number of compression test specimens for each type of column is shown in the penultimate column of Table 7.1, and this number complies with the European standard EN 15512: 2020 (2020), which stipulates that the minimum number of samples must be three. The dimensions of the profile sections were either measured or obtained from technical datasheets (***b, 2019).

Table 7.1. Main dimension values of the Omega-shaped cross-sections of the tested columns and the corresponding yield stress of their material (Dumbrava and Cerbu, 2024)..

No.	Upright type	Design dimensions of the cross section			Measured thickness of the flange t_m (mm)	Yield stress		Number of specimens tested	Coefficient k_s***
		Width W* (mm)	Depth D* (mm)	Thickness t* (mm)		Nominal f_y (MPa)	Measured $f_{y\,exp}$** (MPa)		
1	Type A	85.0	64.8	1.8	1.78	355	384.4	9	1.95
2	Type B	119.0	91.6	2.5	2.51	420	441.3	26	1.74
3	Type C	119.0	91.6	2.5	2.53	420	441.0	5	2.33
4	Type D	88.0	71.4	1.5	3.47	420	425.9	30	1.73
5	Type E	140.5	92.6	3.5	1.53	420	520.0	20	1.76
6	Type F	88.0	71.4	1.5	1.51	420	407.5	10	1.92
7	Type G	99.5	91.6	2.5	2.53	420	534.1	11	1.89
8	Type H	99.5	91.6	2.5	2.53	420	471.7	35	1.72
9	Type I	74.5	66.3	1.5	1.51	420	516.8	3	3.37
10	Type J	60.5	55.0	2.0	2.03	350	353.0	7	2.08
11	Type K	120.0	75.0	2.5	2.60	355	430.8	5	2.33
12	Type L	80.0	68.8	1.8	1.80	280	288.7	8	2.00
13	Type M	84.8	72.8	1.5	1.49	420	427.2	10	1.92
14	Type N	63.0	45.0	1.5	1.50	355	380.0	7	2.08
15	Type O	100.0	82.5	2.0	2.00	355	348.2	8	2.00

*The significance of the cross-sectional dimensions of the columns is shown in Figure 5.2 in Chapter 5.
** Values were obtained from tensile tests performed with the INSTRON 3369 machine.
*** is a coefficient provided in the European standard EN 15512 (2020), selected based on the number of specimens tested in the respective set.

7.1.2. Testing method for determining the critical buckling load of columns

To determine the effective area of Omega-shaped profiles, compression tests were conducted on short columns according to the EN 15512 (2020) standard. The buckling load was measured for each profile, and the average value was used to calculate the effective area. Failure modes and the effects of different dimensions and shapes of perforations on the buckling strength were also analyzed. Test specimens were prepared according to the standard, with a minimum length of three times the profile width and including at least five sets of perforations. Each profile's length was checked to ensure it had a relative slenderness ratio less than 0.2, in accordance with EN 15512 (2020).
The loading scheme for the compression test is shown in Figure 7.3(a), as per the European standard EN 15512 (2020), while Figure 7.3(b) presents a photograph of a column mounted on the device during the compression test.

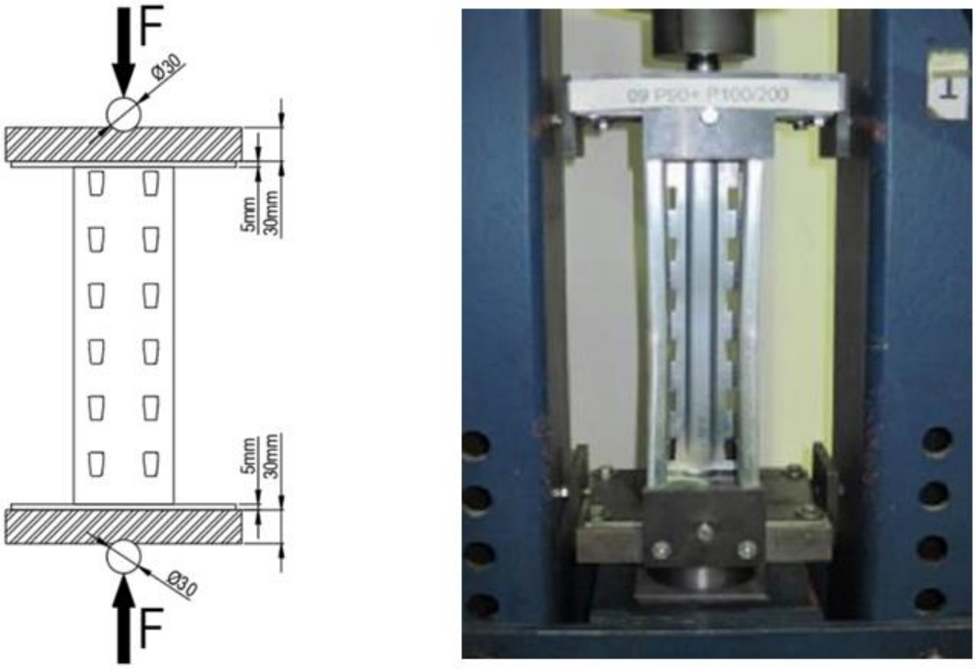

(a) (b)

Figure 7.3. Compression Test Configuration Used to Determine the Buckling Load for Short Columns with Omega-Shaped Cross-Section:(a) Loading scheme; (b) Photograph of a column fixed at both ends on the test bench (Dumbrava and Cerbu, 2024).

7.1.3. Results of the compression testing of columns

In the initial phase of the research, preliminary tests were conducted to identify the optimal position for applying the axial load on the columns to maximize the buckling load. Initially, the axial force was applied at the theoretical center of gravity of the profile without perforations, but later the force application was adjusted by 1-2 mm along the axis of symmetry to account for the perforations. Following these preliminary tests, additional tests were carried out on the number of columns specified in Table 7.1, determining the buckling load for each profile type. The average values of the critical buckling loads, along with the standard deviation, are presented in Table 7.2. These values were corrected according to the EN 15512 (2020) standard to obtain the corrected critical buckling load. Finally, the effective area was calculated for each profile type, and the results are presented in Table 7.2.

Table 7.2. Experimental Results from Compression Tests (Dumbrava and Cerbu, 2024)

No.	Upright type	Average value of the experimental failure forces $F_{exp\,ave}$ (kN)	Stdev s (kN)	Correction coefficient k_s *	*Experimental failure force* F_{exp} ** (kN)	Effective area $A_{eff\,exp}$ (mm²)
1	Type A	124.3	1.53	1.95	121.3	341.7
2	Type B	291.3	3.41	1.74	285.4	679.5
3	Type C	334.7	2.04	2.33	329.9	785.5
4	Type D	447.6	4.39	1.73	440.0	1047.6
5	Type E	121.4	1.94	1.76	117.9	280.7
6	Type F	117.9	1.97	1.92	114.1	271.7
7	Type G	253.9	3.23	1.89	247.8	590.0
8	Type H	259.5	2.47	1.72	255.3	607.9
9	Type I	89.1	1.20	3.37	85.0	202.4
10	Type J	98.4	1.90	2.08	94.4	269.7
11	Type K	204.9	2.91	2.33	198.2	558.3
12	Type L	97.4	0.93	2.00	95.5	341.1
13	Type M	139.1	1.61	1.92	136.0	323.8
14	Type N	82.7	1.15	2.08	80.3	226.2
15	Type O	156.1	1.38	2.00	153.3	431.8

* The correction factor was established according to the European standard EN 15512 (2020).

** This value was corrected according to the European standard EN 15512 (2020).

7.2. Numerical simulation of stress and strain states in compressed storage system columns

The simulation of profile stability loss was performed using RFEM 5.28 software with finite element modeling. The columns were modeled with shell elements, while the end plates were represented with solid elements (Fig. 7.7). Welded connections were simulated using close contact between the upper section of the column and the end plates. Spherical joints were used to restrict movements, except for axial displacement. The model included the nonlinear behavior of steel, employing a bilinear scheme for the stress-strain curve, with an elastic zone limited to the yield stress and a plastic modulus of 2.1 GPa. The analysis also considered geometric nonlinearities.

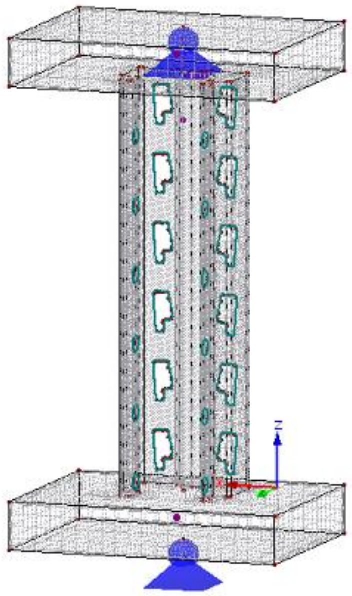

Figure 7.7. Finite Element Model Used for Numerical Simulation of Column Stability Loss (Dumbrava and Cerbu, 2024).

In the numerical model, geometric imperfections were introduced according to the recommendations of the EN 1993-1-5 (2007) standard: (i) for local buckling, the imperfection size was the width of the front part of the column divided by 200; (ii) for distortional buckling, the dimension was the cross-sectional size divided by 50. Additionally, two other imperfections, 15% and 5% of the nominal section thickness, were also considered. The four types of imperfections used in the analysis are: Imp_W/200, Imp_D/50, Imp_0.15t, and Imp_0.05t, and their values are presented in Table 7.3.

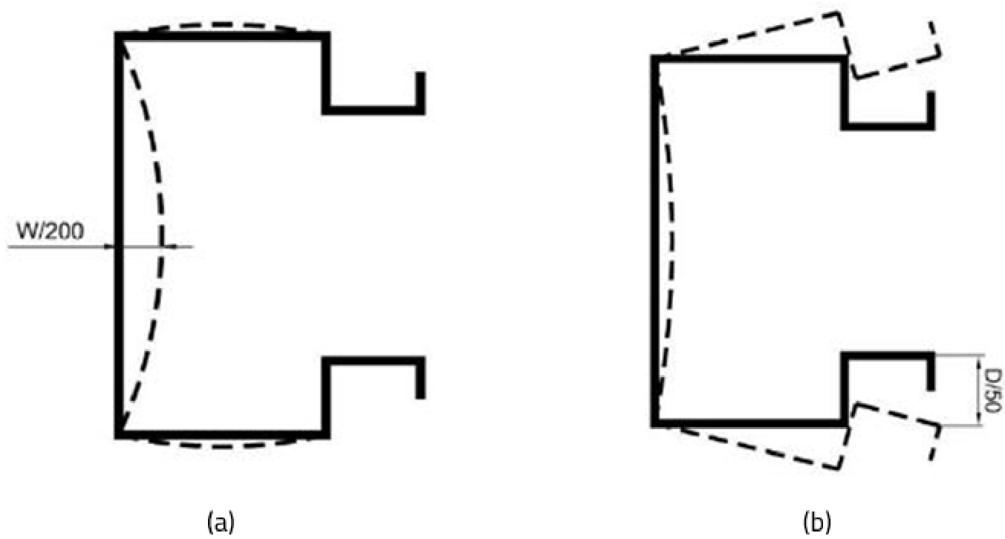

Figure 7.8. Geometric imperfections introduced in the numerical model for the corresponding buckling modes: (a) local buckling; (b) distortional buckling (Dumbrava and Cerbu, 2024).

Table 7.3 Dimensions of geometric imperfections considered for the numerical models used in the analysis of column stability loss (Dumbrava and Cerbu, 2024).

No.	Upright type	Size of the geometrical imperfection (mm)			
		Imp_W/200*	Imp_D/50**	Imp_0.15t***	Imp_0.05t***
1	Type A	0.4250	1.2960	0.2625	0.0875
2	Type B	0.5950	1.8320	0.3750	0.1250
3	Type C	0.5950	1.8320	0.3750	0.1250
4	Type D	0.7025	1.8520	0.5250	0.1750
5	Type E	0.4400	1.4280	0.2250	0.0750
6	Type F	0.4400	1.4280	0.2250	0.0750
7	Type G	0.4975	1.8320	0.3750	0.1250
8	Type H	0.4975	1.8320	0.3750	0.1250
9	Type I	0.3725	1.3260	0.2250	0.0750
10	Type J	0.3025	1.1000	0.3000	0.1000
11	Type K	0.6000	1.5000	0.3750	0.1250
12	Type L	0.4000	1.3760	0.2625	0.0875
13	Type M	0.4240	1.4560	0.2250	0.0750
14	Type N	0.3150	0.9000	0.2250	0.0750
15	Type O	0.5000	1.6500	0.3000	0.1000

** The imperfection is introduced for the local buckling mode.*

*** The imperfection is introduced for the distortional buckling mode.*

*** The imperfection is introduced for the first buckling mode.*

7.3. Validation of the numerical model

In the second phase of the buckling analysis, the geometric imperfections listed in Table 7.3 were considered. According to the EN 1993-1-5 standard, imperfections coded as Imp_W/200 were applied for local buckling, while those coded as Imp_D/50 were used for distortional buckling. The imperfections Imp_0.15t and Imp_0.05t were employed for the first buckling mode of all analyzed profiles. The buckling loads obtained through finite element analysis (FEA) are presented in Table 7.5. The calculated errors compared to the experimental average values for each profile and type of geometric imperfection are also shown in Table 7.5.

Table 7.5. Results from Finite Element Analysis (FEA) for the Numerical Models of Columns, Considering Geometric Imperfections (Dumbrava and Cerbu, 2024)

No.	Upright type	Buckling force F_{FEA} (kN)				Experimental buckling force $F_{exp\,ave}$ (kN)	Error (%)			
		Imp_W/200	Imp_D/50	Imp_0.15t	Imp_0.05t		Imp_W/200	Imp_D/50	Imp_0.15t	Imp_0.05t
1	Type A	115.92	106.68	116.76	118.45	124.3	7.23	16.52	6.46	4.94
2	Type B	273.40	261.45	281.32	286.53	291.3	6.55	11.42	3.55	1.66
3	Type C	306.69	281.91	304.43	309.87	334.7	9.13	18.73	9.94	8.01
4	Type D	407.54	379.54	413.08	417.10	447.6	9.83	17.93	8.36	7.31
5	Type E	112.03	108.13	115.96	116.56	117.7	5.06	8.85	1.50	0.98
6	Type F	115.01	107.34	115.3	115.27	117.9	2.51	9.84	2.25	2.28
7	Type G	262.55	232.16	263.65	264.49	259.8	1.05	11.91	1.46	1.77
8	Type H	262.28	239.22	263.47	265.19	259.5	1.06	8.48	1.51	2.15
9	Type I	89.65	87.08	90.15	90.53	89.1	0.61	2.32	1.16	1.58
10	Type J	96.13	92.05	96.44	100.96	98.4	2.36	6.90	2.03	2.54
11	Type K	190.38	185.58	200.55	203.79	204.9	7.63	10.41	2.17	0.54
12	Type L	88.77	82.69	89.15	89.22	97.4	9.72	17.79	9.25	9.17
13	Type M	132.27	133.47	132.32	134.58	139.1	5.16	4.22	5.12	3.36
14	Type N	77.16	75.68	77.34	77.80	82.7	7.18	9.28	6.93	6.30
15	Type O	147.34	152.60	149.81	154.55	156.1	5.95	2.29	4.20	1.00
					Average values of the errors		5.40	10.46	4.39	3.57

Upon analyzing the average error values (Table 7.5) for all cases concerning the imposed geometric imperfections in the numerical model used for simulating the stability loss of each profile involved in the study, the conclusion is that the lowest average error value corresponds to the imperfection case coded as Imp_0.05t.

For the imperfection coded as Imp_0.05t, Figure 7.14 illustrates the global deformation states and stress states according to the Von Mises criterion for all four types of profiles analyzed. Detailed information on all profile types can be found in the extended doctoral thesis. These stress and deformation states are presented for the maximum recorded reaction force at stability loss, corresponding to the values in Table 7.5 for the imperfection Imp_0.05t.

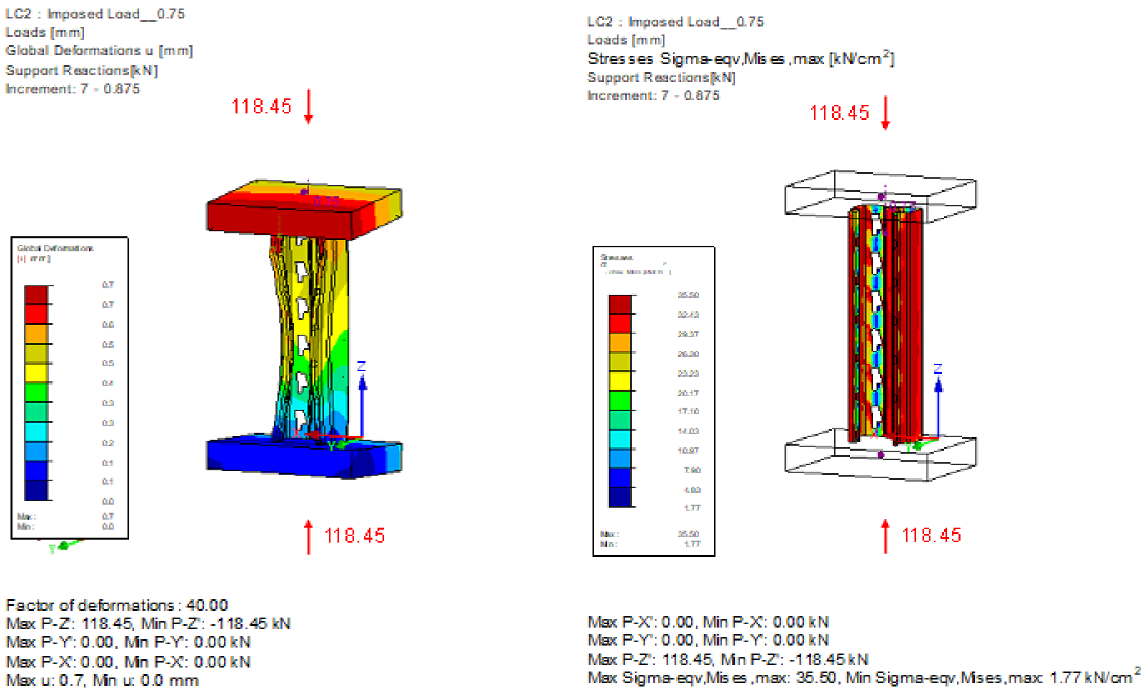

(a1) (a2)

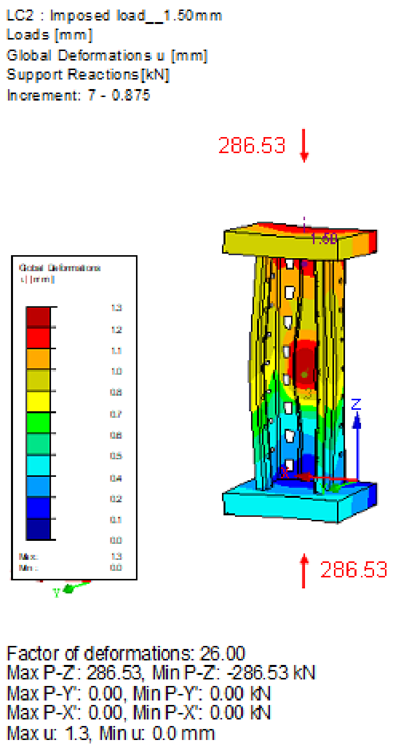

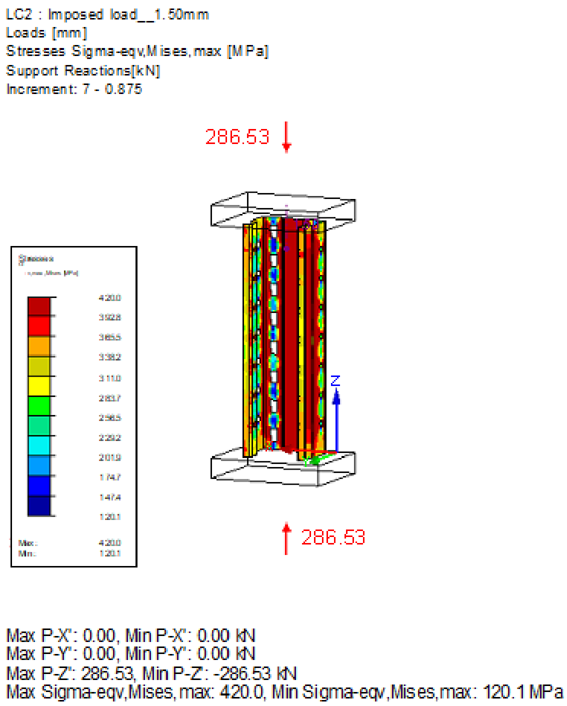

(b1) (b2)

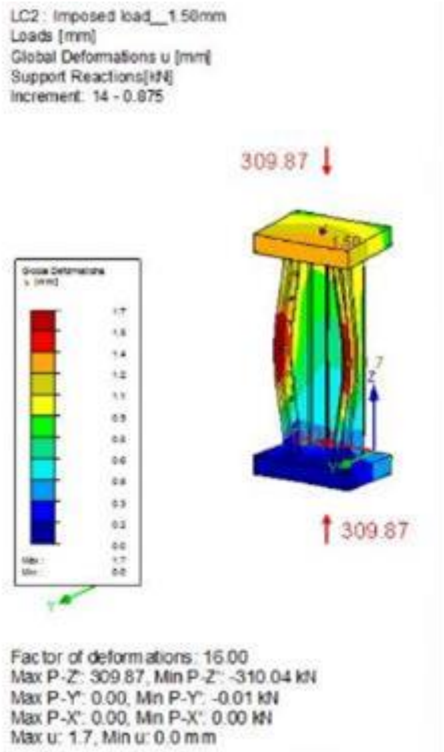

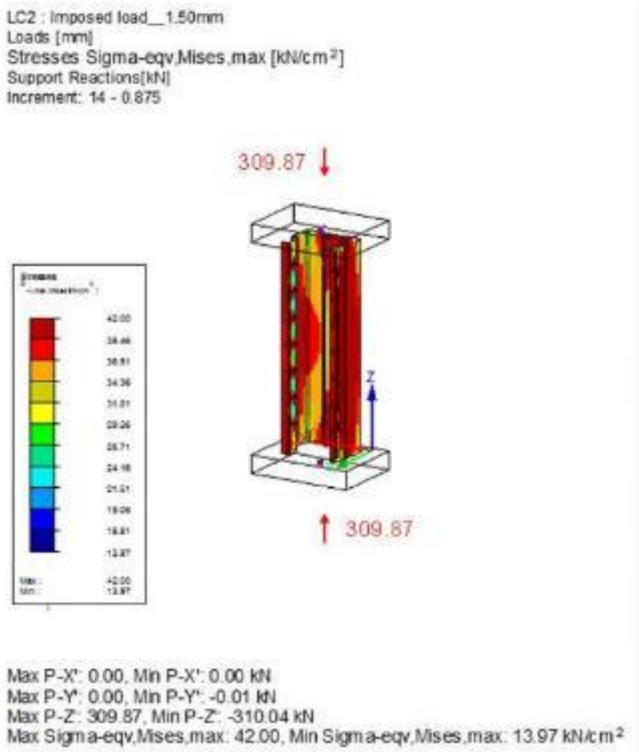

(c1) (c2)

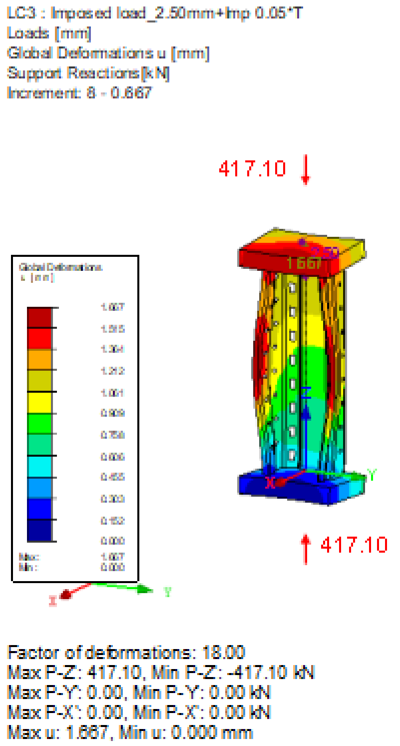

(d1)

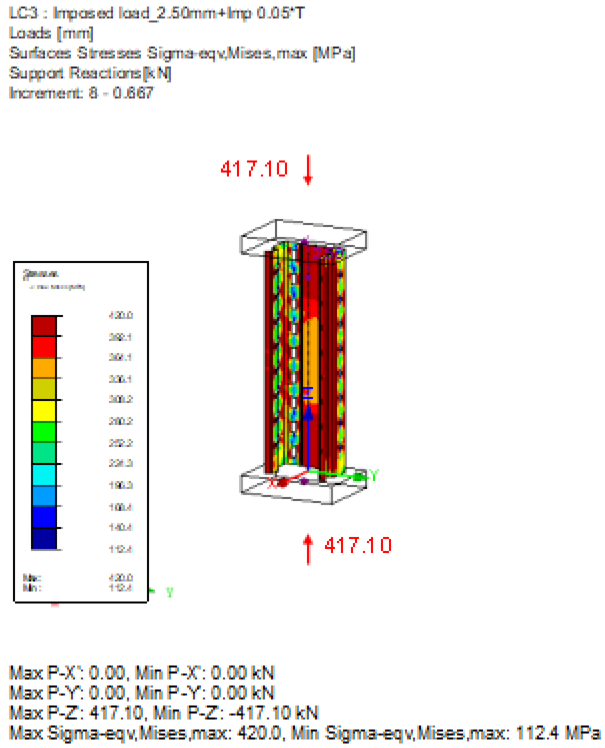

(d2)

Figure 7.14 Global Deformation and Von Mises Stress Distributions for Stability Loss Force, Obtained with FEA, Considering Geometric Imperfections Imp_0.05t for Profiles: (a1), (a2) Type A; (b1), (b2) Type B; (c1), (c2) Type C; (d1), (d2) Type D; (Dumbrava and Cerbu, 2024)

Figure 7.15 compares the failure modes observed in compression tests with those obtained through FEA for two profile types (A, I). Additional cases can be found in the extended doctoral thesis. The results show a high degree of similarity between the experimentally observed failure modes and those numerically simulated.

(a)

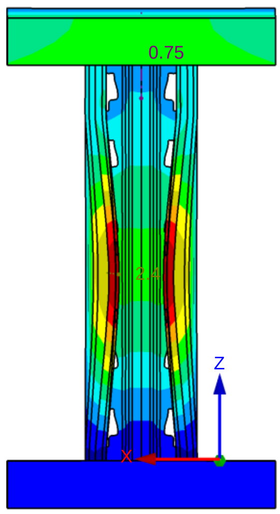

(b)

(c)

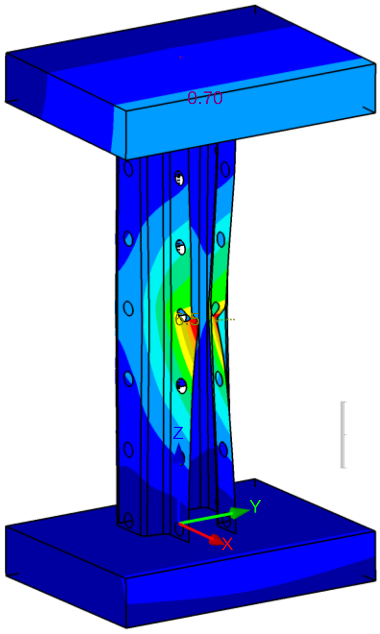

(d)

Figure 7.15. Comparisons between the stability failure modes observed in experiments and those obtained through numerical simulation for the following column profiles: (a, b) Profile type A; (c, d) Profile type I (Dumbrava and Cerbu, 2024).

7.4. Conclusions

The values of critical buckling forces for the tested profiles were obtained through compression tests performed on 15 types of profiles used in the manufacturing of columns in steel storage systems. These tests aimed to validate the numerical model used for simulating these tests. Each column was analyzed using four finite element numerical models, each having different geometric imperfections: the imperfections coded as Imp_W/200 and Imp_D/50, according to the European standard EN 1993-1-5 (2007), as well as the imperfections coded as Imp_0.15t and Imp_0.05t, corresponding to 15% and 5% of the wall thickness *t* of the column profile, respectively. Complete details and the main conclusions of these studies are presented in the full doctoral thesis.

Based on the conclusions obtained from the research presented in this chapter, it is recommended to use geometric imperfections of 5% of the profile thickness in the numerical models that simulate the behavior of columns under compression. This approach will allow for obtaining precise values for the critical buckling force through finite element analysis of the stability loss of perforated columns with Omega-type cross-sections, which are frequently used in pallet rack storage systems.

8. GENERAL CONCLUSIONS. PERSONAL CONTRIBUTIONS. FUTURE RESEARCH DIRECTIONS.

8.1. General conclusions

The research presented in this doctoral thesis focused on two main areas of study: (i) experimental testing of beam-column connections with pin connectors used in pallet racking storage systems; and (ii) theoretical and experimental studies on the local or distortional instability of columns with Omega-shaped cross-sections.

Regarding the study of mechanical behavior of connections, the research extended to the influence of clearances between the metal pins of the connectors and the perforations in the columns on the connector's rotation angle until the clearances are eliminated, as well as the impact on the maximum deflection of the loaded beam and the bending moment at the end of the beam for the considered practical study case.

The studied connections are semi-rigid connections frequently used in pallet racking systems. For the 15 types of beam-column connections, the mechanical behavior of pin connectors fixed at the ends of the beams assembled with the columns was examined, analyzing the influence of the type of connector (four and five pins) and the wall thickness of the profiles used for columns on the rotational stiffness of the connection. Ultimately, the effect of these factors on the load-bearing capacity and the maximum deflection of the beam under mechanical loading was also analyzed.

The diversity of the 15 types of profiles involved in research concerning the stability loss of columns made from thin-walled profiles with Omega-shaped cross-sections, along with the validation of numerical models through comparison of finite element analysis results with experimental results, led to interesting conclusions and personal contributions regarding the magnitude of geometric imperfections to be considered in finite element numerical simulations of stability loss for columns with Omega-shaped cross-sections.

Considering the objectives of the research conducted in this doctoral thesis, the following highlights the main conclusions of this work.

- The results from Chapter 5 show that for assemblies containing Type I columns with a profile thickness of 1.50 mm, the use of a five-pin connector leads to higher values for the design moment capacity M_{Rd} and rotational stiffness k_m compared to using four-pin connectors. In contrast, for Type III columns with a thickness of 2.00 mm, five-pin connectors exhibited slightly lower design moments compared to four-pin connectors.
- For assemblies containing five-pin connectors, the rotational stiffness k_m is approximately 23.1%, 61%, and 77.1% greater than for assemblies containing four-pin connectors for beams of Type A, Type B, and Type C, respectively. Similarly, for assemblies with five-pin connectors, the increase in the design moment M_{Rd} is approximately 49.3%, 21.7%, and 26.5% compared to the values obtained for assemblies with four-pin connectors for beams of Type A, Type B, and Type C, respectively (see Chapter 5).
- It is noted that for the practical study case considered, concerning the beams that support the pallets on the shelves of a storage structure, which have a length of 2.7 m and use the same type of semi-rigid connection at both ends, the rigidity condition according to the European standard EN 15512 (2020) is met for all types of beam-connector-column joints involved in

this research (see Chapter 5.6).

- For the practical study case considered in Chapter 5.6, using Type A and Type C beams, it is found that the best assemblies are A-II-4L and C-II-4L from the perspective of the connection's safety factor c, calculated as the ratio between the design moment capacity M_{Rd} of the connection and the moment at the end of the beam (from the connector), taking into account the rotational stiffness k_m of the connections at the beam end. Furthermore, these types of connections lead to a reduction in the mass of the storage system with shelves, both due to the reduced thickness of the column profile and the use of the four-pin connector. Consequently, this also results in reduced material costs.
- For the same study case considered in Chapter 5.6, it was observed that the ratio between the highest and lowest safety factors is as follows: 1.68 (i.e., the ratio of 4.41/2.63) for assemblies containing Type A beams; 1.69 (the ratio of 4.57/2.70) for assemblies containing Type B beams; and 1.73 (the ratio of 5.94/3.42) for assemblies containing Type C beams. The conclusion is that, for any beam type involved in this research, there is an approximate safety margin of 70%, which depends on the type of connector, the type of column used, and the type of beam employed.
- In Chapter 5.5, it was shown that for beam-connector-column assemblies containing columns made from the thinnest profile, with a thickness of 1.50 mm, the failure mode involves deformation of the perforations on the front side of the column. Other failure modes include: deformation of the connector under bending stress; and local buckling of the beam in the area close to the connector.
- Research on the effects of play between the pins of metal connectors and the perforations in the columns, in the connections between the beam and the column, has led to quantitative results for the rotational displacement Φ_l of the connector (determined when the play in the connection is eliminated). These results show that this value (expressed in radians in Table 6.3) is 1.66 times greater when the beam-connector-column assembly contains a column made from a profile with a wall thickness of 1.50 mm compared to when using a column made from a profile with a wall thickness of 2 mm.
- For the study case considered in Chapter 6.4, based on the experimental results for the rotational displacement Φ_l of the connector (determined when the play in the connection is eliminated), the maximum calculation corrections were 2.99% and 5.16% (Table 6.4) for the bending moment M_{mij} developed at the mid-span of the beam and for the maximum deflection v_{max}, respectively, compared to the case where the effects of play in the connections are ignored.
- It was also concluded at the end of Chapter 6 that the correction values, both for the bending moment M_{mij} developed at the mid-span of the beam and for the maximum deflection v_{max}, are more significant as the column wall with which the beam is connected becomes thinner. Additionally, it is noted that the ratio between the maximum deflection v_{max} of the beam, calculated considering the effects of play between the connector pins and the column perforations, and the maximum deflection in the case where the effects of play are neglected, is greater for the five-pin connector (with a ratio between 1.025 and 1.052) than for the four-pin connector (with a ratio between 1.016 and 1.029).

- The results presented in Chapter 6 demonstrate that design engineers should account for the effects of play in the connections between the beam and the column, made with pin connectors, both in the calculation of the maximum deflection of beams used in pallet racking storage structures and in the calculation of the bending moment developed at the mid-span of the beam, especially for rotational stiffness k_m values of the connection greater than 80 kN·m/rad.
- The theoretical and experimental research presented in Chapter 7, concerning the loss of stability of metal profiles used in the manufacture of columns for storage systems, conducted for 15 different types of profiles, has led to the creation of an extensive database regarding the critical buckling force and effective area, determined through their compression tests.
- The critical buckling forces obtained experimentally match very well with the values obtained through finite element analysis (FEA) when introducing geometric imperfections coded as Imp_0.15t and Imp_0.05t into the numerical model, for the first mode of buckling, with average error values of 4.39% and 3.57%, respectively, for all tested profiles (see Chapter 7.3). However, it was found that for the numerical model with the geometric imperfection coded as Imp_0.05t, the errors exceed 5% (ranging from 6.3% to 9.2%) for only four of the tested profile types: Type C, Type D, Type L, and Type N (see Table 7.5). Additionally, for the numerical model with the imperfection coded as Imp_0.15t, the errors exceed 5% (ranging from 6.4% to 10%) for the following tested profile types: Type A, Type C, Type D, Type L, and Type N.
- Considering both cases of geometric imperfections imposed in accordance with the European standard (EN 1993-1-5 - Eurocode 3 - Part 5, 2007), coded as Imp_W/200 and Imp_D/50, which are recommended for columns without imperfections, it can be observed that the methods for applying these imperfections are suitable only for certain types of tested profiles. For the imperfection coded as Imp_W/200, the best match between the critical buckling force obtained from tests and that obtained through FEA (i.e., with an error less than 5%) was achieved for only half of the total types of columns tested: Type E, Type F, Type G, Type H, Type I, Type J, and Type M (see Chapter 7.3). For the imperfection coded as Imp_D/50, the error is less than 5% only for the following three types of column profiles: Type I, Type M, and Type O (see Chapter 7.3).
- A good match was observed between the modes of failure related to stability loss (local buckling, distortion buckling with opening or closing of the column flanges) obtained from compression tests and those derived from stability loss analysis through numerical finite element modeling (see Chapter 7.3).
- Based on the research results presented in Chapter 7, it is recommended to impose geometric imperfections equal to 5% of the profile thickness in the numerical model simulating the behavior of columns under compression. This is to achieve more accurate values for the critical buckling force, through finite element analysis of the stability loss in perforated columns with an Omega-shaped cross-section.

8.2. Personal contributions

The topic addressed in this doctoral thesis is highly relevant, considering the growing market demand for pallet rack storage systems and the need for continuous improvement in their safety during operation. Both theoretical studies through numerical simulation and experimental investigations have been conducted to analyze the behavior under mechanical loads of key structural elements (beam-to-column connections, column profiles) in these metal storage structures. Numerical models using finite element analysis for evaluating local and distortional buckling of various perforated profiles with an Omega-shaped cross-section have been validated against experimental results.

The following are the author's personal and original contributions in the field of simulation and testing of components in thin-walled metal structures:

- Experimental determination of rotational stiffness and the ultimate bending moment for 18 different types of beam-to-column connections with four- and five-pin metallic connectors was achieved, providing a reference database for engineers and specialists involved in the design of pallet rack storage systems.
- The effects of beam size, profile wall thickness used for columns, and the type of connector (four-pin or five-pin) on the rotational stiffness of the beam-to-column connection were studied, considering the experimentally obtained results.
- Based on experimental results, theoretical comparisons were made of safety coefficients, both regarding the load-bearing capacity of the connection and the stiffness of the mechanically loaded beam with connections at both ends, similar to those investigated in this doctoral thesis. Recommendations were provided for construction variants that best ensure operational safety for such beams.
- Comparative analysis of the maximum deflection and maximum moment developing at the mid-span of the beam with semi-rigid connections at both ends (as considered in the thesis) was performed against cases of double-pin or double-fixed end beams, based on experimental results.
- The importance of considering the behavior of semi-rigid connections by design engineers was justified, as ideal cases of pinned and rigid connections are only theoretical.
- Experimental determination of the rotation angle of the connection until play is eliminated for three types of beam-to-connector-to-column assemblies, varying in profile thickness with an open cross-section used for columns in storage structures.
- The influence of column profile wall thickness on the rotation of the connection until play elimination between the connector's pins and the column was highlighted.
- Experimental results for rotational stiffness were used to theoretically analyze the mechanical behavior of beams with connections at both ends, considering the effects of connection play on the bending moment at mid-span and the maximum deflection.
- The critical buckling force and effective area were determined for 15 different types of profiles used in the manufacture of columns for pallet storage structures, through mechanical testing for local and distortional buckling.
- Numerical models with finite elements were developed for 15 different types of perforated profiles with thin walls and Omega-shaped cross-sections used for storage columns, simulating local and distortional buckling by considering various imperfection cases.
- A comparative analysis of the critical buckling forces for 15 different perforated profiles was performed, obtained through numerical simulation for various imperfection cases in finite element analysis of local and distortional buckling.

- The proposed numerical model for finite element analysis of local and distortional buckling for the 15 different profiles involved in the research was validated by comparing the critical buckling forces obtained numerically with those obtained experimentally.
- A method deemed most appropriate among those studied and validated for the 15 profile types considered in the research was proposed. This method aims to reduce errors between numerical simulation results and experimental results for critical buckling force of local and distortional buckling in the profiles studied. The recommended method may also be applied to other types of perforated profiles with thin walls and open contours for estimating the critical buckling force.
- A comparative analysis of stability loss modes (local or distortional) obtained through numerical simulation versus experimental testing was conducted for the thin-walled perforated profiles involved in the study, leading to further validation of the numerical model.

8.3. Future research directions

The limitations of the study concerning the comparison of four-pin and five-pin metallic connections include the exclusive use of a single cross-sectional profile type for columns and the applicability of the results only at ambient temperature. Future studies should involve diversifying the cross-sectional shapes of columns and developing models adapted for fire conditions.

A promising research direction is investigating the use of Finite Element Analysis (FEA) for evaluating the rotational stiffness of semi-rigid connections with metallic pins. Additionally, analyzing multi-pin connectors and evaluating the stability of storage structures in this context is planned.

Expanding the study to investigate the effects of play in semi-rigid connections with pins would allow for exploring these effects across different cross-sectional profiles for beams made from thin-walled sections.

It is also suggested to extend the use of finite element analysis for studying the nonlinear buckling of Omega profiles and for columns with longer lengths. Accurate measurement of columns used in these studies is crucial to properly assess deviations of profiles from nominal dimensions.

Exploring an equivalent thickness for perforated cross-sections would facilitate the analysis of structures. It is proposed to investigate the possibility of establishing an equivalent thickness for determining the yield strength of Omega-type columns.

BIBLIOGRAPHY

ANSI MH16.1: 2008. Specification for the design, testing and utilization of industrial steel storage racks. In Pallet Beam-to-Column Connection Tests, Rack Manufactures Institute, United States of America: Charlotte, United States of America, 2008; p. 4.

Asl, M.H.; Farivar, B.; Momenzadeh, S. (2019). Investigation of the rigidity of welded shear tab connections. Engineering Structures, 179, pp. 353-366, doi:10.1016/j.engstruct.2018.10.077.

Babeu, T.; Marsavina, L.(1995). Culegere de probleme de rezisten a materialelor. Universitatea Politehnica Timişoara.

Bârsănescu, Paul-Doru (2022). Rezistența materialelor, vol. II, Elemente de stabilitate, elasticitate și solicitări compuse, Editura Tehnopress, Iași, 2022.

Bia, C.; Ille, V.; Soare, M. (1987). Rezistența materialelor şi teoria elasticității. Editura Tehnică, Bucureşti.

Bonada, J.; Pastor, M.M.; Roure, F.; Casafont, M. (2016). Distortional Influence of Pallet Rack Uprights Subject to Combined Compression and Bending. Structures 8, pp. 275-285.

Borkowski, L.; Grudziecki, J.; Kotelko, M.; Ungureanu, V.; Dubina, D. (2022). Ultimate and post-ultimate behaviour of thin-walled cold-formed steel open-section members under eccentric compression. Part II: Experimental study. Thin-Walled Structures, 171, doi: 10.1016/j.tws.2021.108802.

BS EN 10346: 2009. Continuously hot-dip coated steel flat products - Technical delivery conditions. European Committe for Standardization: Brussels, 2009.

BS EN 15512: 2009. Steel static storage systems - Adjustable pallet racking systems - Principles for structural design. European Committe for Standardization: Brussels, 2009.

BS EN ISO 6892-1: 2009. Metallic materials. Tensile testing. Part 1: Method of Test at room temperature. European Committe for Standardization: Brussels, 2009.

Buzdugan, Gh. (1986). Rezistența materialelor. Editura Academiei Romane, Bucureşti.

Cerbu, C. (2014). Strength of materials. Theory and applications; Editura Universitpții Transilvania din Brasov, 398 pagini.

Chou, S.M.; Chai, G.B.; Ling, L. (2000). Finite element technique for design of stub columns. Thin-Walled Structures, 37, pp. 97-112.

Chiriacescu, T. Sergiu; Balcu, Ion (2008). Introducere în teoria elasticității și rezistența materialelor, Editura Universității Transilvania din Brașov, ISBN 978-973-598-244-7, 2008.

Ciofoaia, V. (1987). Rezistența materialelor şi elemente de construcții industriale. Reprografia Universității Braşov.

Ciofoaia, Vasile; Curtu, Ioan (2000). Teoria elasticității corpurilor izotrope și anizotrope, Brașov, 2000.

Coelho, A.M.G.; Bijlaard, F.S.K.; da Silva, L.S (2004). Experimental assessment of the ductility of extended end plate connections. Engineering Structures, 26, pp. 1185-1206, doi:10.1016/j.engstruct.2000.09.001.

Craveiro, H.; Rodrigues, J.P.C.; Laim, L. (2018). Cold-formed steel columns at both ambient and fire conditions. Journal of Structural Fire Engineering, 9, pp. 189-202, doi:10.1108/jsfe-01-2017-0018.

Crisan, A.; Ungureanu, V.; Dubina, D. (2012a). Behaviour of cold-formed steel perforated sections in compression. Part 1-Experimental investigations. Thin-Walled Structures, 61, pp. 86-96.

Crisan, A.; Ungureanu, V.; Dubina, D. (2012b). Behaviour of cold-formed steel perforated sections in compression: Part 2-numerical investigations and design considerations. Thin-Walled Structures, 61, pp. 97-105.

Curtu, I., ş.a. (2000). Rezistența materialelor şi teoria elasticității, partea a III-a, 2000. Reprografia Universității Transilvania din Braşov.

Dai, L.S.; Zhao, X.Z.; Rasmussen, K.J.R. (2018a). Flexural behaviour of steel storage rack beam-to-upright bolted connections. Thin-Walled Structures, 124, pp. 202-217, doi:10.1016/j.tws.2017.12.010.

daSilva, L.S., Simoes, R., Gervasio, H. (2010). *Design of Steel Structures, Eurocode 3: Design of Steel Structures, Part 1-1: General Rules and Rules for Buildings.* Published by ECCS – European Convention for Constructional Steelwork, Eurocode Design Manuals, ISBN (ECCS) 978-92-9147-098-3, Wilhelm Ernst & Sohn Verlag, GmbH & Co. KG, Berlin. SN003a-EN-EU NCCI: *Elastic Critical Moment for Lateral Torsional Buckling.* Access Steel, 2006.

Dai, L.S.; Zhao, X.Z.; Rasmussen, K.J.R. (2018b). Cyclic performance of steel storage rack beam-to-upright bolted connections. Journal of Constructional Steel Research, 148, pp. 28-48, doi:10.1016/j.jcsr.2018.04.012.

Degtyarev, V.V.; Degtyareva, N.V. (2016). Finite element modeling of cold-formed steel channels with solid and slotted webs in shear. Thin-Walled Structures, 103, pp. 183-198, doi:10.1016/j.tws.2016.02.016.

Degtyareva, N.V. (2017). Review of Experimental Studies of Cold-Formed Steel Channels with Slotted Webs under Bending. International Conference on Industrial Engineering, 206, pp. 875-880, doi:10.1016/j.proeng.2017.10.566.

Degtyareva, N.V.; Degtyarev, V.V. (2016). Experimental investigation of cold-formed steel channels with slotted webs in shear. Thin-Walled Structures, 102, pp. 30-42, doi:10.1016/j.tws.2016.01.012.

Deutsch, I. (1979). Rezistența materialelor. Editura Didactică şi Pedagogică, Bucureşti.

Dubina, D. (2010). Contract nr. 424/08.12.2009. Verificarea la stabilitate a elementelor din otel în conformitate cu SR EN 1993-1-1.1. Recomandări de calcul, comentarii si exemple de aplicare. Timisoara 2010.

Dubina, D.; Ungureanu, V. (2023). Local/distortional and overall interactive buckling of thin-walled cold-formed steel columns with open cross-section. Thin-Walled Structures, 182, doi: 10.1016/j.tws.2022.110172.

Dumbrava, F.; Cerbu, C. (2020a). Experimental Study on the Stiffness of Steel Beam-to-Upright Connections for Storage Racking Systems. Materials, 13 (13), Article Number: 2949, doi: 10.3390/ma13132949.

Dumbravă, F.; Cerbu, C. (2020b). Analysis of pallet storage structures in down-aisle direction. Proceeding of The 8th International Conference on Advanced Composite Materials Engineering COMAT 2020 & The 3rd International Conference on Experimental Mechanics in Engineering, Brașov, ROMANIA, 29-31 October 2020, ISSN 2457-8541, pp. 49-54. Link conferinta: https://sites.google.com/view/comatcomec/home

Dumbrava, F.; Cerbu, C. (2022a). Effect of the Looseness of the Beam End Connection Used for the Pallet Racking Storage Systems, on the Mechanical Behavior of the Bearing Beams. Materials 15(14), Article Number: 4728, doi: 10.3390/ma15144728.

Dumbrava, F.; Cerbu, C.; Ursache, S. (2022b). Research concerning to the rigidity of the screw joint between beam and column in metal structures, Procedings of The 9th International Conference on Advanced Composite Materials Engineering (COMAT), Brasov, 17 – 18 October, 2022, ISSN 2457 – 8541, ISSN – L2457 – 8541, pp. 66 – 71.

Dumbrava, Florin; Cerbu, Camelia (2024). Local and distortional buckling behaviour of omega-shaped short columns used in pallet racking storage systems: experimental study and numerical modelling, revista Structures (Q1/ 2023, FI: 3.9/ JCR 2023, ISSN: 2352-0124). Manuscript ID: STRUCTURES-D-24-03235, înregistrat în data de 9 mai 2024, este în curs de recenzie.

Elza, M.M.; Fonseca, L.S.; Pedro A.S. (2020). Numerical model to predict the effect of wood density in wood–steel–wood connections with and without passive protection under fire. Journal of Fire Sciences, 38, pp. 122-135, doi:10.1177/0734904119884706.

EN 15512: 2020. Steel static storage systems - Adjustable pallet racking systems - Principles for structural design. European Committe for Standardization, Brussels.

EN 1993-1-3: 2006. Eurocode 3 - Design of steel structures - Part 1-3: General rules - Supplementary rules for cold-formed members and sheeting. European Committe for Standardization, Brussels.

EN 1993-1-5: 2007. Eurocode 3 - Design of steel structures - Part 5: Piling. European Committe for Standardization, Brussels.

EN ISO 6892-1: 2009. Metallic materials. Tensile testing. Part 1: Method of Test at room temperature. European Committe for Standardization, Brussels.

Escanio, L.A.; Elias, G.C.; Neiva, L.H.D.; Alves, V.N.; Sarmanho, A.M.C. (2020). Analysis of beam-to-upright end connections steel storage systems. Advanced Steel Construction, 16, pp. 279-286, doi:10.18057/ijasc.2020.16.3.9.

Galeotti, C.; Gusella, F.; Orlando, M.; Spinelli, P. (2021). On the seismic response of steel storage pallet racks with selective addition of bolted joints. Structures, 34, pp. 3806-3817, doi:10.1016/j.istruc.2021.10.001.

Gharebaghi, R.; Hosseini, A. (2017). Local behavior of column-tree connections with considering bolt-hole clearance and bolt pretension effects. International Journal of Steel Structures, 17, pp. 379-388, doi:10.1007/s13296-017-6002-z.

Gilbert, B.P.; Rasmussen, K.J.R. (2010). Bolted moment connections in drive-in and drive-through steel storage racks. Journal of Constructional Steel Research, 66, pp. 755-766, doi:10.1016/j.jcsr.2010.01.013.

Godley, M.H.R.; Beale, R.G. (2001). Analysis of large proprietary access scaffold structures. Proceedings of the Institution of Civil Engineers-Structures and Buildings, 146, pp. 31-39.

Goia, Ioan (2002). Mechanics of Materials, 1st vol.,Derc Publishing House, Tewsbury, Massachusetts, USA, ISBN-13 978-0-9817300-0-4, ISBN-10 0-9817300-0-0

Grondin, G.Y.; Jin, M.; Josi, G. (2007). Slip Critical Bolted Connections — A Reliability Analysis for Design at the Ultimate Limit State, University of Alberta: Edmonton, Alberta, Canada, Volume: Structural engineering report SER 270 | SER-ID SER270, doi:10.7939/R3QR4NQ55

Gusella, F.; Arwade, S.R.; Orlando, M.; Peterman, K.D. (2019). Influence of mechanical and geometric uncertainty on rack connection structural response. Journal of Constructional Steel Research, 153, pp. 343-355, doi:10.1016/j.jcsr.2018.10.021.

Gusella, F.; Lavacchini, G.; Orlando, M. (2018). Monotonic and cyclic tests on beam-column joints of industrial pallet racks. Journal of Constructional Steel Research, 140, pp. 92-107, doi:10.1016/j.jcsr.2017.10.021.

Gusella, F.; Orlando, M.; Thiele, K. (2018). Evaluation of rack connection mechanical properties by means of the Component Method. Journal of Constructional Steel Research, 149, pp. 207-224, doi:10.1016/j.jcsr.2018.07.021.

He, Z.Q.; Cao, H.Y.; Zhou, X.H.; Li, Q.X.; Schafer, B.W. (2022). Performance of cold-formed C-sections reinforced by sleeves under concentric and eccentric compression. Journal of Constructional Steel Research, 198, doi:10.1016/j.jcsr.2022.107554.

Huang, S.Q.; Chen, J.; Jin, W.L. (2011). Numerical investigation and design of thin-walled complex section steel columns. Journal of Zhejiang University-Science A, 12, pp. 131-138.

Iliescu, N.; Jiga, G.; Hadăr, A. (1999). Teste – grilă de rezistența materialelor. Editura Printech. Bucureşti, 1999.

Jovanovic, D.; Zarkovic, D.; Vukobratovic, V.; Brujic, Z. (2019). Hysteresis model for beam-to-column connections of steel storage racks. Thin-Walled Structures, 142, pp. 189-204, doi:10.1016/j.tws.2019.04.056.

Kotelko, M.; Grudziecki, J.; Ungureanu, V.; Dubina, D. (2021). Ultimate and post-ultimate behaviour of thin-walled cold-formed steel open-section members under eccentric compression. Part I: Collapse mechanisms database (theoretical study). Thin-Walled Structures, 169, doi:10.1016/j.tws.2021.108366.

Kulak, G.L.; Fisher, J.W.; Struik, J.H.A. (1987). Guide to Design Criteria for Bolted and Riveted Joints, 2nd Edition ed.; Editura John Wiley & Sons: New York.

Laim, L.; Rodrigues, J.P.C. (2018). Fire design methodologies for cold-formed steel beams made with open and closed cross-sections. Engineering Structures, 171, pp. 759-778, doi:10.1016/j.engstruct.2018.06.030.

MECALUX - Warehouse Storage Solutions. Fire protection measures for metal racks and warehouses. Availabe online: https://www.mecalux.com/logistics-items/fire-protection-measures-for-metal-racks-and-warehouses (accessed on 23.06.2020).

Marșavina, L. (2206). Metode experimentale de determinare a tenacită ii la rupere, Ed. Politehnica, Timişoara, 205 pag.

Mohan, V.; Prabha, P.; Rajasankar, J.; Iyer, N.R.; Raviswaran; N.; Nagendiran, V.; Kamalakannan, S.S. (2015). Cold-formed steel pallet rack connection: an experimental study. International Journal of Advanced Structural Engineering (IJASE), 7, pp. 55–68, doi:10.1007/s40091-015-0082-9.

Mourya, U.; Jayachandran, S.A. (2022). Finite element model-based dynamic characteristic predictions for cold-formed steel storage racks. In Proceedings of the Proceedings of the Annual Stability Conference Structural Stability Research Council, Denver, Colorado, March 22-25, 2022; pp. 1-9.

Năstăsescu, V.; Bîrsan, Gh. (1997). Rezistența materialelor – Probleme, vol.I şi II. Editura Academiei Tehnice Militare, Bucureşti.

Năstăsescu, V.; Bârsan, G. (2021). Elasticitate și plasticitate. Capitole speciale. Editura Academiei Forțelor Terestre „Nicolae Bălcescu", Sibiu, ISBN: 978-973-153-429-9.

Oeztuerk, F.; Mojtabaei, S.M.; Sentuerk, M.; Pul, S.; Hajirasouliha, I. (2022). Buckling behaviour of cold-formed steel sigma and lipped channel beam-column members. Thin-Walled Structures, 173, doi:10.1016/j.tws.2022.108963.

Peiris, M.; Mahendran, M. (2021). Behaviour of cold-formed steel lipped channel sections subject to eccentric axial compression. Journal of Constructional Steel Research, 184, doi:10.1016/j.jcsr.2021.106808.

Prabha, P.; Marimuthu, V.; Saravanan, M.; Jayachandran, S.A. (2010). Evaluation of connection flexibility in cold formed steel racks. Journal of Constructional Steel Research, 66, pp. 863-872, doi:10.1016/j.jcsr.2010.01.019.

Prabhakaran, U.; Beale, R.G.; Godley, M.H.R. (2011). Analysis of scaffolds with connections containing looseness. Computers & Structures, 89, pp. 1944-1955, doi:10.1016/j.compstruc.2011.03.016.

Roșca, Ioan Călin (2020). Rezistența materialelor, partea I, Editura Universității Transilvania din Brașov, ISBN 978-606-19-1335-0-4.

Roure, F.; Pastor, M.M.; Casafont, M.; Somalo, M.R. (2011). Stub column tests for racking design: Experimental testing, FE analysis and EC3. Thin-Walled Structures 49(1), pp. 167-184, doi:10.1016/j.tws.2010.09.002.

Sanborn, M.; Stewart, L.K. (2020). Behavior of slip-critical bolted connections subjected to impulsive loads. International Journal of Impact Engineering, 143, Article Number: 103501, doi:10.1016/j.ijimpeng.2020.103501.

Schabowicz, K. (2021). Testing of Materials and Elements in Civil Engineering. Materials, 14(12), Article Number: 3412, doi:10.3390/ma14123412.

Shah, S.N.R.; Sulong, N.H.R.; Shariati, M.; Khan, R.; Jumaat, M.Z. (2016). Behavior of steel pallet rack beam-to-column connections at elevated temperatures. Thin-Walled Structures, 106, pp. 471-483, doi:10.1016/j.tws.2016.05.021.

Shariati, M.; Tahir, M.M.; Wee, T.C.; Shah, S.N.R.; Jalali, A.; Abdullahi, M.M.; Khorami, M. (2018). Experimental investigations on monotonic and cyclic behavior of steel pallet rack connections. Engineering Failure Analysis, 85, pp. 149-166, doi:10.1016/j.engfailanal.2017.08.014.

Singh, T.G.; Chan, T.M. (2021). Effect of access openings on the buckling performance of square hollow section module stub columns. Journal of Constructional Steel Research, 177, doi:10.1016/j.jcsr.2020.106438.

Ślęczka, L.; Kozłowski, A. (2008). Design of beam-to-column joints in steel storage pallet racks by testing and by component method, Archives of Civil Engineering, LIV(1), pp. 263-291.

Soare, M., ş.a. (1996). Rezistența materialelor în aplicații. Editura Tehnică. Bucureşti, 1996.

Talebian, N.; Gilbert, B.P.; Miller, D.; Karampour, H. (2022). Biaxial bending design of solid steel storage rack uprights in global buckling. Journal of Constructional Steel Research, 196, doi:10.1016/j.jcsr.2022.107395.

Timoshenko, S.P.; Gere, J.M. (2009). Theory of elastic stability, Second edition. Dover ed. ISBN-13: 978-0-486-47207-2, ISBN-10: 0-486-47207-8.

Ungureanu, V.; Both, I.; Kotelko, M.; Czechowski, L.; Bodea, F.; Dubina, D. (2022). Buckling strength and post-ultimate behaviour of lipped channel section short columns under eccentric compression. Thin-Walled Structures, 181, doi:10.1016/j.tws.2022.110085.

Vincent, N.K.; Varghese, A.; Ajeesh, S.S. (2023). Distortional-Global Interactive Buckling of Thin-Walled Columns with Complex Lips. International Journal of Steel Structures, 23(4), pp. 945-961, doi:10.1007/s13296-023-00740-4.

Yazici, C.; Arik, E.; Özkal, F.M., (2023). Influence of design parameters on beam-to-column connections of steel storage rack systems. Engineering Failure Analysis, 152, doi:10.1016/j.engfailanal.2023.107439.

Yin, L.F.; Tang, G.; Zhang, M.; Wang, B.J.; Feng, B. (2016). Monotonic and cyclic response of speed-lock connections with bolts in storage racks. Engineering Structures, 116, 40-55, doi:10.1016/j.engstruct.2016.02.032.

Yu, N.T.; Kim, B.; Yuan, W.B.; Li, L.Y.; Yu, F. (2019). An analytical solution of distortional buckling resistance of cold-formed steel channel-section beams with web openings. Thin-Walled Structures, 135, pp. 446-452, doi:10.1016/j.tws.2018.11.012.

Zadanfarrokh, F.; Bryan, E.R. (1992). Testing and Design of Bolted Connections in Cold Formed Steel Sections. In Proceedings of the International Specialty Conference on Cold-Formed Steel Structures. 3., Missouri University of Science and Technology, 1992, https://scholarsmine.mst.edu/isccss/11iccfss/11iccfss-session11/3.

Zhang, J.F.; Wang, B.; Wang, S.; Deng, E.F.; Zhang, P.; Pang, S.Y.; Wen, M.G.; Ye, L.; Guo, X.S.; Gao, J.L. (2021). Eccentric compressive distortional buckling and design of non-symmetric cold-formed angular column with complex edges. Thin-Walled Structures, 165, doi:10.1016/j.tws.2021.107981.

Zhang, P.; Alam, M.S. (2020). Elastic buckling behaviour of Sigma-shaped rack columns under uniaxial compression. Engineering Structures, 212, Article Number: 110469, doi:10.1016/j.engstruct.2020.110469.

Zhao, X.Z.; Dai, L.S.; Wang, T.; Sivakumaran, K.S.; Chen, Y.Y. (2017a). A theoretical model for the rotational stiffness of storage rack beam-to-upright connections. Journal of Constructional Steel Research, 133, pp. 269-281. doi:10.1016/j.jcsr.2017.02.014.

Zhao, X.Z.; Ren, C.; Qin, R. (2017b). An experimental investigation into perforated and non-perforated steel storage rack uprights. Thin-Walled Structures, 112, pp. 159-172, doi: 10.1016/j.tws.2016.11.016.

Zhao, X.Z.; Dai, L.S.; Wang, T.; Sivakumaran, K.S.; Chen, Y.Y. (2017). A theoretical model for the rotational stiffness of storage rack beam-to-upright connections. Journal of Constructional Steel Research, 133, pp. 269-281, doi:10.1016/j.jcsr.2017.02.014.

Zhao, X.Z.; Wang, T.; Chen, Y.Y.; Sivakumaran, K.S. (2014). Flexural behavior of steel storage rack beam-to-upright connections. Journal of Constructional Steel Research, 99, pp. 161-175, doi:10.1016/j.jcsr.2014.04.007.

Zhong, W.H.; Tan, Z.; Tian, L.M.; Meng, B.; Song, X.Y.; Zheng, Y.H. (2020). Collapse resistance of composite beam-column assemblies with unequal spans under an internal column-removal scenario. Engineering Structures, 206, doi:10.1016/j.engstruct.2019.110143.

Zhou, T.H.; Li, Y.C.; Ren, L.J.; Sang, L.R.; Zhang, L. (2021). Research on the elastic buckling of composite webs in cold-formed steel back-to-back built-up columns - Part I: Experimental and numerical investigation. Structures, 30, pp. 115-133, doi:10.1016/j.istruc.2020.12.059.

***a, Cataloage de prezentare a produselor, Dexion Storage Solutions SRL (Râșnov), 2019.

***b, Documentație tehnică referitoare la dimensiunile și caracteristicile geometrice ale secțiunii grinzilor produse pentru sistemele de depozitare, cu rafturi pentru paleți, Dexion Storage Solutions SRL (Râșnov), 2019.